The Effects Of Titanium On Submerged-arc Weld Metal.

SNYDER, JAMES P., II

THE EFFECTS OF TITANIUM ON SUBMERGED-ARC WELD METAL

Lehigh University PH.D. 1980

PLEASE NOTE:

In all cases this material has been filmed in the best possible way from the available copy. Problems encountered with this document have been identified here with a check mark ✓.

1. Glossy photographs ✓
2. Colored illustrations _____
3. Photographs with dark background ✓
4. Illustrations are poor copy _____
5. Print shows through as there is text on both sides of page _____
6. Indistinct, broken or small print on several pages _____ throughout _____
7. Tightly bound copy with print lost in spine _____
8. Computer printout pages with indistinct print _____
9. Page(s) _____ lacking when material received, and not available from school or author _____
10. Page(s) _____ seem to be missing in numbering only as text follows _____
11. Poor carbon copy _____
12. Not original copy, several pages with blurred type _____
13. Appendix pages are poor copy _____
14. Original copy with light type _____
15. Curling and wrinkled pages _____
16. Other _____

THE EFFECTS OF TITANIUM ON SUBMERGED-ARC WELD METAL

By

James P. Snyder, II

A Dissertation

Presented to the Graduate Committee

of Lehigh University

in Candidacy for the Degree of

Doctor of Philosophy

in

Metallurgy and Materials Engineering

Lehigh University

1980

CERTIFICATE OF APPROVAL

Approved and recommended for acceptance as a dissertation in partial fulfillment of the requirements for the degree of Doctor of Philosophy.

May 14, 1980
(date)

Alan W. Perce
Professor in Charge

Accepted May 14, 1980
(date)

Special committee directing the doctorial work of James P. Snyder, II

Alan W. Perce
Chairman

DEDICATION

This work is dedicated to my wife, Judi and my daughter, Meredith without whose patience, understanding, encouragement, and prayers.....

ACKNOWLEDGEMENTS

The author would like to express his sincere appreciation to all who contributed their efforts to the completion of this dissertation. Especial acknowledgements are due his advisor, Dr. A. W. Pense, and the members of his PhD examining committee for their encouragement and helpful advice throughout the study.

The author is grateful to the Bethlehem Steel Corporation for the use of the facilities of the Homer Research Laboratories and the sponsorship of the author through graduate school at Lehigh University. Acknowledgements are also due to many of the author's co-workers including Messrs. Bauer, Benscoter, Brandemarte, and Kilpatrick for their skillful assistance and patience in educating an armchair metallurgist in the ways of hands-on technology.

TABLE OF CONTENTS

LIST OF FIGURES

LIST OF TABLES

ABSTRACT

The effects of titanium on the mechanical properties and microstructure in the submerged-arc weld deposit of high-strength low-alloy silicon-aluminum-killed low-sulfur steels containing various amounts of titanium were determined. The titanium was introduced into the weld via dilution from the base plate. The nominal carbon, manganese, silicon, and titanium ranges in the weld deposits were 0.05-0.15, 1.0-1.4, 0.35-0.60, and 0.0-0.15% respectively. Most of the welding was done with carbon-manganese electrodes. But some welds were made with carbon-manganese-molybdenum and carbon-manganese-molybdenum-nickel electrodes to determine the contribution of electrode composition to toughness. The effect of flux basicity was also determined.

Yield and tensile strengths were obtained from all-weld-metal tensile specimens. Toughness data were determined with standard Charpy specimens. Various microstructural features found in the weld deposits were identified and quantified by means of optical and electron metallography.

The data were statistically analyzed using factorial designs based on carbon, manganese, silicon, and titanium. Equations were developed to predict mechanical properties for compositions within the design limits.

Generally, yield and tensile strengths correlated well with

carbon, manganese, silicon, and titanium. Yield strengths ranged from 449 to 535 MPa and tensile strengths ranged from 570 to 648 MPa. As titanium increased, both the yield and tensile strengths increased. The toughness was strongly dependent on titanium and manganese content, while carbon and silicon had smaller effects. Toughness ranged from 5 J at -46 C to 106 J at +52 C. Titanium reduced toughness by increasing the maximum weld hardness through solid solution hardening and also by increasing the amount of ferrite veining at low-manganese levels. Manganese improved toughness by reducing the amount of ferrite veining and by refining the microstructure.

Weld metal toughness was also improved by use of higher basicity fluxes and electrodes containing molybdenum or molybdenum plus nickel. The fluxes reduced the weld oxygen level with a concomitant reduction in inclusion volume. The molybdenum and molybdenum plus nickel additions reduced the ferrite veining.

The results of this study demonstrate that although titanium is detrimental to the toughness of submerged-arc welds, its deleterious effects can be offset by proper selection of welding consumables.

INTRODUCTION

In the past ten years four approaches have been used to obtain high strength and improved toughness in high-strength low-alloy (HSLA) weldable steels:[1]

1. using controlled alloying,
2. alloying with carbide- or nitride-forming elements to obtain grain-refinement and precipitation hardening,
3. lowering the carbon content below 0.1% to improve toughness and weldability, and
4. alloying to change the shape or size of sulfides to improve the isotropy of toughness properties.

If these measures are implemented jointly, several alloying elements must normally be added to the steel. These joint additions may bring about disadvantages because not all of the precipitation-harding and sulfide-controlling elements are compatible with each other.

Titanium has been found to act both as a strengthening and sulfide-controlling element. These properties of titanium have not been extensively capitalized upon because the effects of titanium, alone or in combination with other alloying elements, on precipitation and weldability are not well understood. Indeed a literature survey yielded little information on the effects of titanium as the sole alloying addition on the weldability of HSLA steels. A considerable

number of papers have dealt with titanium in conjunction with columbium and/or vanadium in regards to weldability. HSLA steels microalloyed with columbium and/or vanadium have been agressively marketed in almost all steel producing countries thus supplying the impetus to achieve an understanding of their weldability.[2-11] However, as columbium and vanadium are about two and one-half times more expensive than titanium for an equal alloy recovery, economics mandate a closer examination of titanium as a sole microalloying addition and in particular its effect on weldability.

The construction of pipelines for gas and oil has been accelerated by our increasing comsumption of energy. The demands for high fuel flow rates have led to increased pipe diameters and thicknesses and higher operating pressures. Much of the gas and oil reserves are in harsh environments with limited accessibility. Thus the strength and toughness requirements for the steel are strict to insure reliability and safety. The ability of the new HSLA steels to meet these requirements has made them attractive for the linepipe and offshore oil markets. Since a large portion of the welding in these markets is done with the submerged-arc process, a study into the effects of titanium on submerged-arc weld metal would be beneficial to the steel and pipeline industries.[12]

Titanium Effects in HSLA Steel Welds

Several studies have indicated that small titanium additions improve the Charpy toughness of multipass welds. A number of authors have quoted 0.04% titanium as the optimum addition to carbon-manganese weld metals. Smaller titanium additions were required for more highly alloyed deposits.[6,13-21] The conclusion from these studies is that the optimum level reflects a balance between the grain-refining and hardening effects of titanium.

Patchett, et.al., found that the fracture resistance was continuously reduced by titanium additions in single pass CO_2-shielded, gas-metal-arc welds.[22] They reported a yield strength increase of 60 MPa and an increase of the 0.1 mm crack-opening-displacement transition temperature of 63°C by a 0.1% titanium addition to the weld deposit. Borisenko and Navozkilov working with titanium additions to electrodes questioned whether optimum titanium levels could be achieved in practice with adequate reliability. Because of the low and variable transfer efficiency of titanium, variations in chemistry result.[23] They felt that was no adverse effect of small amounts (0.04% maximum) of titanium pickup from titanium-bearing steels.

Widgery found that titanium in excess of 0.04% in the weld deposit reduced toughness by solid solution hardening and by

promoting coarser microstructures.[14] He theorized that the powerful ferrite forming action of titanium increases the amount of proeutectoid ferrite which results in an increase in the transition temperature.

Similar effects of titanium up to the 0.1% level were reported by Kotecki and Moll[24] and also by Bauman, et.al.[6] The solution-hardening effect of titanium is almost certainly a contributory factor,[25] and the resulting decrease in toughness associated with weld metal titanium contents above 0.04% is also in agreement with the work of Boniszewski.[15]

In contrast to the work just reported, several studies have found that titanium suppresses proeutectoid ferrite (ferrite veining) formation in the weld metal and thereby enhances toughness up to an optimum level of titanium. Ito and Nakaniski have suggested that acicular ferrite rather than proeutectoid ferrite is formed by titanium nitride particles acting as nuclei for the intragranular growth of the ferrite plates.[13] The toughness improvement they reported was theorized to be due to a reduction in the mean free path for propagating cracks, which was attributed to a reduction in proeutectoid ferrite. The embrittling effect of proeutectoid ferrite results not from any inherent brittleness of this structure, but from its "mortar-in-brickwork" morphology.[26]

Boniszewski also noted that high toughness was associated with grain refinement.[15] He deduced that some critical amount of titanium is associated with maximum notch toughness. Below the critical amount, titanium increases toughness by it's grain-

refining action. The addition of titanium in excess of the critical amount, 0.04%, caused solid solution hardening of the ferrite which was said to override the beneficial effects of the grain refinement.

The contradictions surrounding the role of titanium in the weld deposit lie in the differences of welding conditions, processes, and materials used in the various studies. It is believed that titanium has varying effects depending on the type and quantity of other elements present in the weld. Since carbon, manganese, silicon, and oxygen are typically found in weld deposits and are variables in this study, it is instructive to examine the literature in their regard.

Carbon Effects in Weld Metal

As-deposited weld-metal yield and tensile strengths are increased as carbon is increased. Carbon increases the transition temperature and lowers the absorbed energy of a Charpy curve and has been shown to be deleterious to submerged-arc welds.[27-29] In some commercial weld deposits, however, optimum Charpy V-notch results were obtained at about 0.08% carbon. The lower carbon contents were believed to cause coarser structures with lower impact resistance. While carbon may have a detrimental influence on toughness of equivalent microstructures, carbon may in some cases alter microstructures to make them tougher and more desirable.[30,31]

Generally, carbon above 0.08% increases the strength and

decreases the notch toughness of weld deposits by increasing the proportion of carbides in the microstructure or by promoting low-carbon martensite.[32,33]

Manganese Effects in Weld Metal

Widgery found that manganese promoted the formation of acicular ferrite and decreased the proportion of proeutectoid ferrite, increased the strength and lowered the transition temperature.[14] These changes were linear with increasing manganese over the range of 0.4 to 1.6% in the weld metal. Similar results were found by Sakaki in increasing manganese up to 1.1%.[34] Dorschu and Stout found that as manganese was added to the weld deposit the hardness was increased and the ferrite grain size decreased.[28] Tuliani and Farrar found that manganese in the range of 1.2 to 1.4% improved the microstructure by promoting acicular ferrite and decreasing proeutectoid ferrite which increased the toughness over lower manganese deposits.[32] Sagan and Campbell found that increasing manganese up to about 2% had a favorable influence on notch toughness.[30]

Silicon Effects in Weld Metal

Silicon's role has been questionable. A number of authors have reported a deterioration in toughness with silicon contents above 0.3%.[35,36] Hughes however, shows an improvement in microstructure and toughness of submerged-arc welds as silicon

was increased up to 0.52%.[37] Tuliani and Farrar suggest a silicon content of 0.18% for optimum toghness.[32] Stout and Moll found that silicon first decreased and then increased the transition temperature.[29] Sakaki found little effect in submerged-arc welds on adding silicon up to 0.50%.[34] Results similar to Sakaki's were obtained by Dorschu and Stout and also by Wilms.[38] Widgery found that the effects of silicon were weak and ill-defined over the range of 0.17 to 1.2%.[14]

Oxygen Effects in Weld Metal

Oxygen content in a submerged-arc weld is primarily dependent upon the type of flux chosen. Generally, fluxes with a basicity index less than one (known as an acid flux) will produce welds with higher oxygen contents (>0.06%) than fluxes with basicity indexes of one or greater. The latter produce welds with low oxygen contents (<0.04%). Neutral fluxes (basicity indexes of about one) will result in oxygen in the 0.04 to 0.06% range [39-41]

Kirkwood has shown that the majority of low-carbon weld metals deposited under low-oxygen potential fluxes exhibit acicular ferrite microstructures unless some other powerful bainite promoting element is present.[7] Higher oxygen weld metals (>0.04%) on the other hand, will tend to be upper bainitic in character unless significant amounts of alloying with elements such as molybdenum and nickel are employed. The extent of alloying necessary to promote acicularity in such a case could result in

excessive solid solution strengthening and thus embrittlement. Molybdenum and nickel are effective in reducing the amount of proeutectoid ferrite and promoting an acicular structure.[2,42,43] To counter the strength increase obtained when using these two elements, limitations on carbon and manganese content may be necessary.[41]

Microconstituents in Weld Metal

The three main components seen in weld deposits are proeutectoid ferrite, acicular ferrite, and grain boundary ferrite with a lath morphology.[3,44,46,47] While it is believed that these microconstituents can be broadly classified, the quantitative measurement of these features is difficult. An uncertainty arises because the constituents are three dimensional colonies and the polished surface of the specimen is a random plane through them. A given microstructural feature appears with a variety of morphologies and can be difficult to recognize in some orientations. Also, polishing and etching techniques become very important in quantitative metallography.

Levin and Hill have introduced a simplified method for classifying weld metal microstructures.[44] Their classification system is comprised of two categories: Category I consists of welds whose structure contains grain boundary ferrite and interior acicular ferrite; Category II consists of welds in which the grain boundary boundary ferrite has been replaced by growth of a structure which has a lath morphology. The latter structure

is thought to originate primarily from prior austenite grain boundaries; it dominates the Category II weld metal.

Although the trend has been to stress that good weld deposit toughness can be produced by simply avoiding proeutectoid ferrite in favor of acicular ferrite, results by Signes show the situation is by no means that simple.[8,43] He shows two microstructures that appear to be identical, yet one structure produces a high absorbed energy and the other, a low energy. Garland and Kirkwood have made a similar point, i.e., that avoiding proeutectoid ferrite by no means ensures high weld metal toughness.[45]

Summary of the Literature

Summarizing the literature, it appears that for good toughness a weld deposit should have a carbon content of 0.08%, a manganese content of 1.3%, a silicon content of 0.30%, a titanium content of 0.04%, and an oxygen content of 0.04%. The desired microstructure is one which has a majority of acicular ferrite and a minimum of proeutectoid ferrite or Levin's Category II structure of lath morphology. Additions of molybdenum and nickel can be used to promote the desired microstructure while a basic flux can produce the low oxygen content.

MATERIALS

A set of twenty-one 227 kg laboratory ingots were poured and rolled to 13 mm thick plate. The chemistries of these plates are given in Table 1. The compositions of plates 1 thru 9 are based upon a two-level three-factorial design around carbon, silicon, and titanium at a nominal manganese level of 1.45%.[48,49] Plates 10 to 13 were based on a 0.20% titanium level. Plates 14 to 18 were made to fit a partial factorial design around carbon, manganese, and titanium at a nominal silicon level of 0.45%. Plates 19 to 21 were added to extend the titanium content in the first factorial design. Several of the heats provided base material for both series.

Three commercially produced submerged-arc welding electrodes, 4 mm in diameter, were used in this study. The electrode chemistries are given below:

Electrode	C	Mn	P	S	Si	Mo	Ni	Ti	Al
123	0.12	1.97	0.012	0.024	0.03	0.004	0.04	0.004	0.008
128	0.15	1.89	0.011	0.017	0.05	0.50	0.05	---	0.035
130	0.16	1.91	0.006	0.013	0.07	0.42	0.84	0.004	0.008

The three commercially produced welding fluxes used in this study had the following chemistries:

Flux	SiO_2	Al_2O_3	TiO_2	CaO	MgO	MnO	FeO	Na_2O	CaF_2	BI*
85	39.3	5.5	18.6	20.7	0.4	13.0	0.9	0.05	2.2	0.59
851	42.8	2.6	11.5	37.5	0.4	0.4	0.4	0.05	4.5	0.85
0091	34.1	3.0	4.2	43.9	0.4	0.4	0.2	4.80	9.3	1.55

*BI (Basicity Index[39]) = $\dfrac{(CaO+CaF_2+MgO+K_2O+0.5(MnO+FeO))}{(SiO_2+0.5(Al_2O_3+TiO_2+ZrO_2))}$

A majority of the welds were made with electrode 123 and flux 85. Electrodes 128 and 130 were used to determine the effect of adding molybdenum or molydbenum plus nickel on the weld metal properties. Flux 851 and 0091 were used to determine the effect of flux basicity on weld metal properties.

EXPERIMENTAL TECHNIQUES

The experimental program is outlined below:

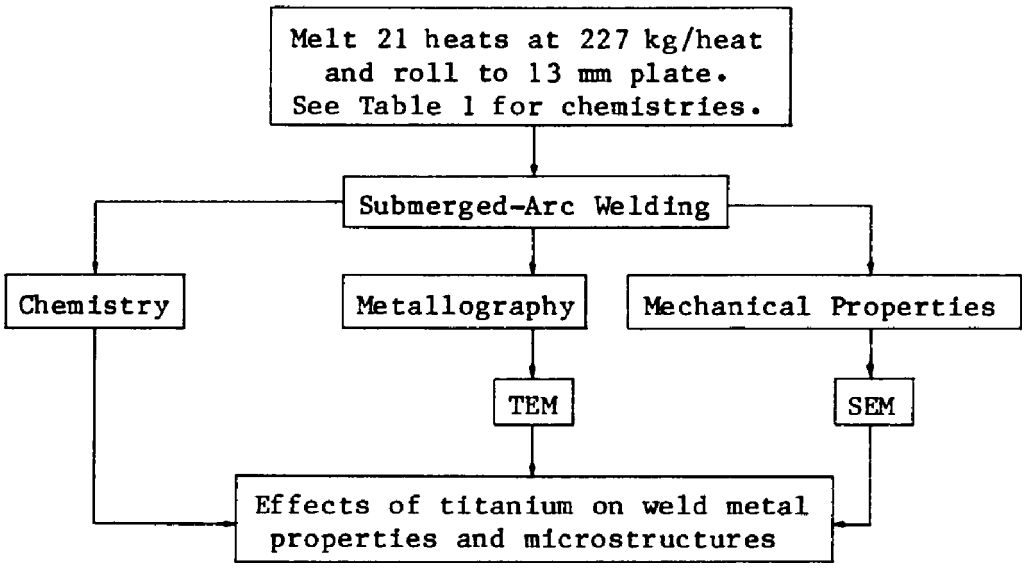

An oxygen-acetylene cutting torch was employed to cut the plates in half longitudinally. Starting and stopping tabs were tack welded to the ends of the plates as shown in Figure 1. A Scott-connected, tandem AC submerged-arc welding process was used to produce full penetration welds of one pass per side in 13 mm thick plate. The following welding parameters were used:

Parameter	Lead Arc	Trail Arc
Current	900 amperes	600 amperes
Voltage	35 volts	40 volts
Travel Speed	163 cm/min.	163 cm/min.
Energy Input	11.6 kJ/cm	8.9 kJ/cm
Total Energy Input	20.5 kJ/cm	

Figure 2 shows the orientation of the welding electrodes. An arc spacing of about 16 mm and an electrode stickout of about 30 mm

were utilized. The trail electrode was inclined about 15 degrees away from the lead electrode. These conditions added titanium into the weld deposit via dilution from the base plate. Table 2 lists the weld deposit chemistries.

Cooling rates were obtained from several of the welds by harpooning W-5%Re versus W-26%Re thermocouples into the molten weld pool just in back of the trail electrode. Cooling rates for ten such measurements had a mean value of 11.0°C/sec. between 800 and 500 C with a standard deviation of 0.5°C/sec.

Specimens were removed for tensile and Charpy testing and chemical analysis as indicated in Figure 1. Full-size Charpy specimens were obtained transverse to the welding direction and notched in the plate thickness direction so as to contain about 60% of the second weld bead and about 40% of the first weld bead as shown below.

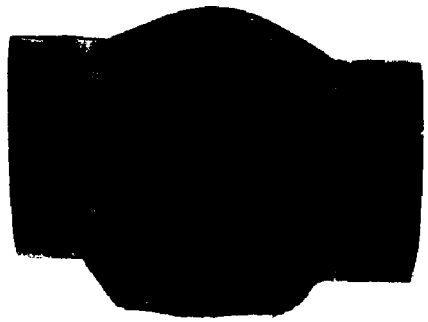

All-weld-metal tensile specimens were taken from the second weld bead in the longitudinal direction. The figure below shows the placement of the tensile specimen.

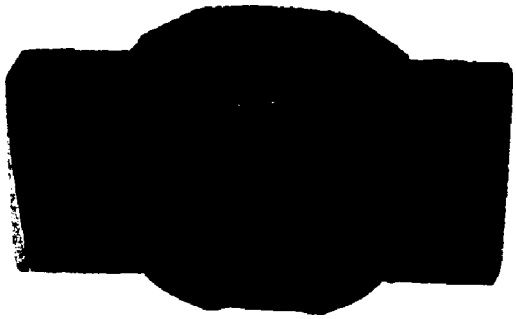

gage length = 12.7 mm

gage diameter = 3.2 mm

Specimens for metallography and hardness testing were final polished with 0.03 micron aluminum oxide powder and etched in 2% nital unless otherwise indicated. Quantitative metallography was accomplished by using a Leitz Texture Analysis System and also by optical point counting. The Leitz system uses approximately 260000 picture points per field of view for its analysis while the manual counting used 100 points per field of view. The following measurements were made:

1. Volume fraction of proeutectoid ferrite
2. Volume fraction of non-metallic inclusions
3. Volume fraction of retained austenite
4. Grain size of acicular ferrite
5. Grain size of polygonal ferrite in the reheated zone of the first weld bead

On selected samples, retained austenite was measured by x-ray diffraction as a check on the optical measurements. The amount

was measured using the ratio of the gamma (111) and (200) x-ray peaks to the alpha (110) peak.[50] A G.E. XRD-5 diffractometer was used with vanadium-filtered chromium K-alpha radiation and a 45 KV excitation voltage.

Specimens for transmission electron microscopy (TEM) were primarily taken from the second weld bead and mechanically polished to 0.38 mm, chemically thinned to 0.05 mm in 5% hydrofloric acid 30% hydrogen peroxide in water followed by electro-jet thinning in 10% perchloric acid in acetic acid at 12 C.

The fracture surfaces of broken impact specimens were examined on the scanning electron microscope (SEM).

Qualitative analysis of inclusions was determined using the electron microprobe (EMP).

PRESENTATION AND DISSCUSION OF RESULTS

Statistical Analysis

The first objective of this research was to determine the influence of titanium, carbon, manganese, and silicon on mechanical properties and microstructure. The second objective was to determine the relationship, if any, between microstructure and mechanical properties.

In the following presentation, plate chemistry, flux and electrode chemistry, and the welding process and parameters are considered to be independent variables. Since, of these, only plate chemistry was varied it is assumed to be the prime independent variable for the main portion of the study. With a constant dilution factor of the base metal into the weld deposit, the weld chemistry becomes the prime independent variable due to the relationship between the base plate and weld deposit chemistries. To eliminate any problems concerning variable dilutions, the statistical analyses were based on the weld deposit chemistries.

Titanium dilution was determined using two techniques; chemistries and area measurements. Figure 3 shows the titanium dilution to be about 50% as determined from weld and base metal chemistries. A 67% dilution was calculated from area measurements. The cross-hatched area below is divided by the total fused metal area to obtain the percent dilution. In this calculation, the

area ratio is assumed to be in the same proportion as the volume ratio.

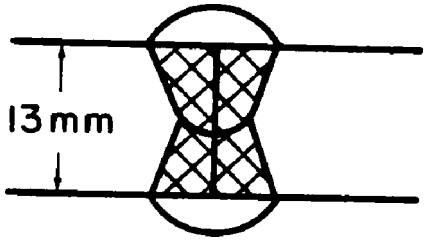

The discrepency between the titanium and area dilutions is due to the loss of titanium to the slag via oxidation.

The mechanical properties and microstructures are assumed to be dependent on chemistry. But among these it is assumed that properties are also secondarily related to the microstructure. This assumption is supported by much work correlating the two in steel. However, the properties and microstructures may not be singularly related.[51] For example, a steel can be subjected to various heat treatments to produce a fine pearlite, a mixture of ferrite and martensite, or a tempered martensite, all of which display identical hardness, but which possess distinct differences in toughness. Similarly, two steels of different compositions can be heat treated to identical hardness, perhaps even by the same cooling method yet their microstructures and properties will be different. Signes found a similar situation when comparing properties and microstructures of weld deposits.[8] In one case he had two welds of different compositions with identical microstructures, yet one displayed poor toughness (20 J at -46 C) while the other weld displayed high toughness (129 J at -46 C).

With these thoughts in mind, the hierarchical relationships among the various parameters can be represented as shown below. The thickness of the arrows indicates the relative weights assumed to exists among weld chemistry, microstructure, and properties.

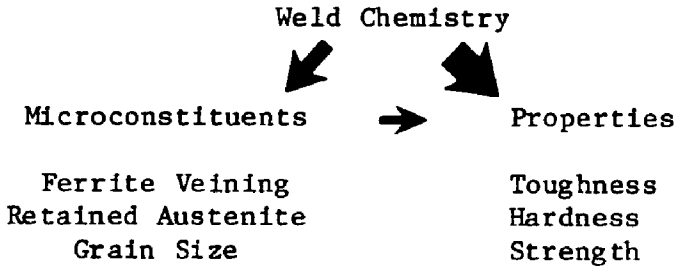

In this study two factorially designed series of welds were tested. The first series, the CTS series, was based on variations in carbon, titanium, and silicon levels at a nominally constant manganese level. The second series, CTM, was based on variations in carbon, titanium, and manganese levels at a nominally constant silicon level. The weld groupings and respective elemental ranges for both series are shown in Table 3.

Factorial designs were employed because they permit estimation of the effects of several factors simultaneously. Both main effects and interactions of the prime variables can be estimated. This is converse to a classical design, i.e., one-factor-at-a-time experimentation, where information is obtained for only a single variable and interactions are assumed to be negligible. Also, factorial designs are economical from a number of trials per unit information basis.[48]

To establish the effect of the independent variables on the

dependent variable the following general relationship was assumed to exist:

$$\text{secondary variable} = B_0+B_1X_1+B_2X_2+B_3X_3+ B_{11}(X_1)^2+B_{22}(X_2)^2+B_3(X_3)^2+ B_{12}(X_1X_2)+B_{23}(X_2X_3)+B_{13}(X_1X_3)$$

where B_n is the coefficient of the independent variable X_n. The last three terms were included to account for possible interactive effects of the independent variables. The independent variables to be substituted into the above equation for X_n are carbon, titanium, and silicon for the CTS series and carbon, titanium, and manganese for the CTM series.

The data were fit to the equation using a regression program which generated the coefficients, the multiple correlation coefficient (R) and the standard error of the estimate (SErr).[52] The P-tail (P), i.e., the percent of the variability explained by chance, was calculated for each equation with a program developed by Hewlett-Packard.[53] The results can be found on Table 4. In the last colume of Table 4, a correlation is defined as excellent if the P of the equation is <0.01, good if $0.01<P<0.05$, fair if $0.05<P<0.15$, and poor for $P>0.15$. Another way of looking at the P statistic is if P of an equation is equal to 0.02, than it can be said that the relationship

expressed by the equation has two chances out of one hundred of having occured by chance.[49]

Since a ten-coefficient equation is not easily grasped, a series of graphs based on the regression data was plotted. For each dependent variable, nine graphs of predicted isolevels of that variable were plotted. Carbon was held constant at 0.06, 0.09,and 0.12% in three of the nine graphs and isolevels were plotted on graphs of titanium versus silicon or titanium versus manganese depending on whether CTS or CTM data were used. Similarly, isolevels were plotted for fixed contents of 0.01, 0.085, and 0.16% titanium, 0.35, 0.475, and 0.60% silicon, and 1.0, 1.2, and 1.4% manganese. In all, 234 graphs were made, to aide in the understanding of the regression equations. Several of these graphs are presented in the following section.

Chemistry Effects on Mechanical Properties

The mechanical properties to be discussed are toughness, hardness, and strength. Data are given in Tables 5, 6, and 7. Figures 4 to 12 present the results of the statistical analyses discussed above. These figures were selected to graphically illustrate the most important effects of composition on mechanical properties discovered in this research.

Figure 4 shows that titanium strongly increases and manganese strongly decreases the 55 joule transition temperature. Figures

5 and 6 show that carbon and silicon, respectively have little effect on the transition temperature. Similar curves were found for the 20 joule transition temperature. Titanium and manganese have strong effects on absorbed energy as shown in Figure 7 for -18 C. Carbon and silicon again have little effect on absorbed energy. Generally where they do have an effect, carbon is detrimental while silicon is beneficial to toughness. Figure 8 shows the effect of carbon on absorbed energy at -18 C while Figure 9 shows the silicon effect at -32 C.

Maximum weld hardness was raised by increasing the carbon, titanium, and manganese contents. Silicon had no well-defined effect.

The yield and tensile strengths were increased by additions of carbon and titanium. Silicon raised the yield strength but had a slight effect on the tensile strength. Manganese on the other hand had only a slight effect on the yield strength but increased the tensile strength. These trends are shown for tensile strength in Figures 10, 11, and 12 Figure 10 shows the tensile strength increasing with increasing carbon and titanium. Figure 11 shows tensile strength increasing with manganese and carbon. Figure 12 shows silicon to have little effect on tensile strength.

Charpy V-Notch Energy

The strength of a factorial design is that it gives both main effects and interactions. The analyses showed that the strongest

effects on toughness were caused by titanium and manganese, with the carbon and silicon having only minor effects. Thus concentration was turned to the effects of titanium and manganese.

Titanium was found to correlate well with the absorbed energy at all test temperatures, for both high (1.3%) and low (1.05%) manganese levels. Figure 13 shows that as titanium increases, the toughness at -46 C decreases. Also note that the lower manganese data points show lower toughness values than the higher manganese points. Data points on the graph are actual points from Tables 2 and 6. The same two trends of titanium decreasing and manganese increasing the toughness are evident at -18 C and +52 C as shown in Figures 14 and 15 respectively. The 20 and 55 joule transition temperatures shown in Figures 16 and 17 respectively, increase with increasing titanium and decreasing manganese contents.

Weld Metal Hardness

The titanium trend found in the preceeding five figures is partially explained in Figure 18. Here, the maximum weld hardness (Vickers with a 5 kg load) increases with titanium content. This result is consistant with the findings of Boniszewski[15] and Bauman.[6] They concluded that the titanium is affecting the toughness of the weld deposit by increasing the hardness through solid solution hardening with an accompanying decrease in ductility. Note that manganese increases the hardness as its level is raised in Figure 18.

Figure 19 shows the relation between maximum hardness and the

absorbed energy at +24 C. The toughness deteriorates as the hardness increases. The same trend is shown for the transition temperatures in Figures 20 and 21. Thus, titanium has a definite effect on the maximum hardness which can be attributed to a solid solution hardening or possibly to a precipitation effect.

The above results concerning titanium, toughness, and hardness have been supported by the work of Thaulow.[54] In his work to correlate Charpy toughness with fracture toughness, Thaulow used additions of titanium as a means to change the weld deposit toughness. Figure 22 shows Thaulow's data plotted for welds that were made in 30 mm plate with a 96 kJ/cm energy input and a flux having a basicity index of 0.56 (close to that of flux 85 of this study). The results show similar relationships to those found in the present study, namely, as the titanium content of the weld increases the toughness decreases and the hardness increases.

Chemistry Effects on Microstructure

Four microstructural features were examined to explain the variations in toughness. They were: % ferrite veining, % retained austenite, % inclusions, and ferrite grain size (acicular and weld heat-affected zone). Not all of these microconstituents were measured or statistically analyzed for each weld. Tables 7 and 8 list the data.

Ferrite Veining

Of all the transformation products found in carbon-manganese weld deposits, proeutectoid ferrite or ferrite veininig is the most unambiguously recognized. Figure 23A shows a micrograph at 100X of ferrite veining. This veining surrounds areas of harder transformation products, mainly acicular ferrite, which form at lower temperatures[47] and concentrates strain in the ferrite veins. Figure 23B shows acicular ferrite and a small area of ferrite veining (arrow). It is in these veins that cracks often initiate during Charpy testing. Microhardness measurements* given below show the acicular ferrite to be harder than the proeutectoid ferrite.

Weld	Acicular Ferrite	Proeutectoid Ferrite Vein
W058	201	154
S062	265	227

*hardnesses were taken using a 10 gm load and have the units kg/mm^2.

Figure 24 shows the path of crack propagation to be through the ferrite veins.

The ferrite veining was decreased by adding carbon and manganese and can be explained by the increased amount of acicular ferrite produced by these elements. These trends can be seen on Figures 25 and 26. Figure 25 shows the carbon trend and Figure 26 the manganese trend. Silicon had little effect.

Titanium, however, had differing effects depending on the level of manganese. The titanium effect was ill-defined at

the higher manganese contents. In contrast, at lower manganese levels a definite relation exists showing that as titanium increases, the amount of ferrite veining increases. This effect is shown in Figure 27. Figure 28 shows the increase of veining decreasing the absorbed energy at +24 C, and thus is detrimental to toughness. The effect of the ferrite veining may be also coupled with the adverse effect of increased hardness as was shown previously in Figure 18.

The explanation for the different behavior of titanium at high and low manganese levels is believed to lie in the continuous cooling diagrams for these welds. The continuous cooling diagrams that may explain the difference are those determined during post-solidification cooling and not those from classical reheating techniques. This distinction in diagram determination is important because heat-treated weld microstructures are different from as-welded (as-cast) structures. Figure 29 shows the as-cast structure (A) and the reheated structure (B) from the first weld bead of weld W058. These two structures demonstrate that different transformation events took place during cooling. Although no work was done in this area, the following hypothesis is proposed for the observed behavior of titanium.

From classical continuous cooling transformtion data it is known that manganese is an austenite stabilizer and promotes the formation of lower transformation products by shifting the start of transformation curve to the right essentially leaving

the phase fields unchanged.[55,56] Titanium, however, is a ferrite stabilizer and promotes the formation of proeutectoid ferrite by shifting the start of transformation curve to the left and also increases the size of the ferrite field.[57] Abson and Dolby in determining continuous cooling diagrams during post-solidification cooling have found that manganese pushes the curve to the right and also increases the acicular ferrite region within the overall ferrite field.[47] Titanium was felt to increase the proeutectoid ferrite region in the overall ferrite field thus allowing more time to form ferrite veining during cooling. The veining was found to nucleate before the acicular ferrite and hence the proeutectoid region lies above the acicular region.

Figure 30 shows four hypothetical continuous cooling diagrams derived from post-solidification cooling. The proeutectoid ferrite field ($p\alpha$) of diagram A is smaller than the $p\alpha$ of diagram B. Note that the acicular ferrite field ($a\alpha$) is about the same for A and B. Since the cooling rate will be the same for all welds made under identical conditions, the enlarged $p\alpha$ field of B allows more time for transformation to proeutectoid ferrite than in A. Upon increasing the manganese at low titanium, the start of transformation curve of A is shifted to the right and the $a\alpha$ field is enlarged as shown in C. Thus for the same cooling rate more time is spent in the $a\alpha$ field in C than in A and less time is spent in the $p\alpha$ field in C than in A. Comparing D with C, the $p\alpha$ field of D is enlarged and

slightly more time is spent in the $p\alpha$ field of D than in C, but a similar amount of time is spent in the $a\alpha$ field. Thus there is not much change in volume of proeutectoid ferrite at the high manganese level as titanium is increased, however at the low manganese level there is a considerable increase.

Although a hypothesis, this explanation is offered to rationalize the observed results. Similar observations by Levin and Hill tend to support the above hypothesis.[44] They attempted to develop data similar to continuous cooling transformation data by quenching samples directly after welding. Although their technique must be improved to obtain more detailed and precise data, it is believed that similar experiments of this nature could be used to test the hypothesis.

Structure Size

Both titanium and manganese are known to refine the microstructures of steels, but they also can affect the weld deposit in a similar fashion.[20] This is definitely the case for manganese as shown on the two micrographs at 500X in Figure 31. The higher manganese deposit (31B) has a finer microstructure than the lower manganese deposit (31A). The compositions are similar except for manganese. According to Levin and Hill's classification,[44] Figure 31B would be a category I structure due to the acicular ferrite present and 31A would be a category II structure due to the lathlike morphology of the proeutectoid ferrite and the reduced amount of acicular ferrite.

The higher-manganese welds have a finer grain size in the weld heat-affected zone as listed on Table 8. It was not possible to measure the grain size or lath size of the acicular ferrite in the low-manganese welds, due to the coarseness and increased volume of the proeutectoid structure. Titanium did not seem to have a well-defined effect on the ferrite grain size of either the acicular or reheated ferrite. Although a "grain size" or mean intercept length was determined for the welds listed on Table 8, it is felt that quantitative analysis of lath size is not as yet practical for acicular ferrite. All work and equations for grain size have been based on an equiaxed grain.[60] Acicular ferrite laths are not equiaxed and therefore may invalidate the equiaxed analysis. Until the quantitative techniques are further refined, a more qualitative measurement or rating such as a fine or coarse estimation of structure relative to another should be used.

Retained Austenite

Volume fraction of retained austenite was measured in welds of both series. No meaningful correlation was found between this constituent and chemistry. However, in the CTM series there appeared to be a slight correlation with manganese; as manganese increased, retained austenite increased. A similar relation between retained austenite and manganese has been found by Alasaarela.[59] It is believed that the retained austenite measured in this study has little

effect on the properties of the weld deposits due to the small volumes present; the highest volume fraction was 3.8% for weld S091.

Non-Metallic Inclusions

No correlations were found between chemistry and volume of non-metallic inclusions. Qualitative analysis showed the inclusions to be predominately oxides with some sulfides. Since the oxygen and sulfur contents of the welds were essentially constant at 0.08 and 0.01% respectively, the amount of inclusions would be expected to remain constant; nominal amount was 0.6%

Mechanical Properties as Affected by Chemistry and Microstructure

The data sets from both the CTS and CTM series were combined to determine the effects of chemistry and microstructure on the properties of the weld deposits. The 20 and 55 joule transition temperatures, maximum hardness, and the yield and tensile strengths were correlated with carbon, manganese, silicon, titanium, ferrite veining, and retained austenite according to the following equation:

$$\text{Dependent Variable} = B_0 + B_1(C) + B_2(Mn) + B_3(Si) + B_4(Ti) + B_5(\%V) + B_6(\%RA)$$

The results of the analysis are shown in Table 9.

The findings are the same as found in the individual series analysis, but now simpler equations have been developed and include the metallographic data. The veining was again found to decrease both the toughness and strength properties. The toughness was decreased by the veins serving as the preferred path of crack propagation as shown previously in Figure 24. The relationship between strength and veining is based on the relative amounts of high and low strength materials. Figure 32 shows that as the amount of softer veining increases the tensile strength decreases.

The retained austenite had no effect on the dependent variables and therefore did not appear in the equations. The retained austenite is felt not to be detrimental in small amounts. The literature warns however that larger amounts can be deleterious to weld toughness.[35]

The amount of inclusions was not placed into the analysis due to the relative constant amount present. However, as will be pointed out in a later section, toughness can be improved by decreasing the amount of non-metallic inclusions in the weld deposit.

Grain size is believed to be an important factor in the properties as shown in Figure 31; a finer microstructure has better toughness. As was previously mentioned, this measurement was impractical for a majority of the welds and thus was not entered into the analysis.

Evidence Against A Precipitation Mechanism

The relationship between increased hardness and decreased toughness in a weld has been attributed to a precipitation hardening mechanism by various authors.[5,8,16] This explanation has been proposed, but no precipitates were found during electron microscopic examination. Although this explanation is plausible, a lack of hard evidence leaves openings for other interpretations.

It was thought that the relationship between titanium and hardness might be explained by the formation of fine titanium compounds, i.e., carbides or nitrides. However, efforts to find particles to account for the observed property changes were fruitless. Transmission electron microscope work, both thin foil and extraction replicas, yielded no particles except for iron carbides that were associated with fine pearlite throughout the deposit. An attempt was made to extract particles by dissolving the matrix, collecting and x-ray analyzing the residue.[60,61] The only particles found by this technique were oxides which were also quantified in the inclusion measurements. Typically a hardness increase is found where a precipitation hardening mechanism is active due to the aging that occurs in the first weld deposit from the heat of the second weld pass. Hardness traverses made from the second weld bead into the first weld bead showed no evidence of increased hardness as shown for weld S071 in Figure 33.

For these reasons it is concluded that a precipitation mechanism is not active in a major sense in the welds of

this study and that the deleterious effect of titanium is due mainly to solid solution hardening.

Effect of Flux Variations

For line pipe welding, acid fluxes have been popular because they produce sound, smoothly contoured deposits and have good operating characteristics at high current levels and travel speeds typical of the application.[39,40,62] Unfortunately, acid fluxes produce high oxygen contents in the weld metal which is deleterious to notch toughness. Therefore, welds were studied that were produced with three fluxes of varying basicity. A basicity index (BI) is typically calculated for fluxes using the following equation developed by the Welding Institute:[39]

$$BI = \frac{(CaO+CaF_2+MgO+K_2O+0.5(MnO+FeO))}{(SiO_2+0.5(Al_2O_3+TiO_2+ZrO_2))}$$

Figure 34 shows the Charpy energy curves for the three fluxes used to weld plate T109. It is seen that as the basicity of the flux increases the absorbed energy increases, especially

near the upper shelf. Table 10 and Figure 35 show the oxygen content of the weld deposit decreases as the flux basicity increases, which is consistent with the findings of Takahashi.[42] From this relationship it was inferred that the higher basicity flux should contain fewer non-metallic inclusions owing to less oxygen available to form oxides. The volume fraction of non-metallic inclusions was measured for the three welds and the data are presented on Figure 36. As the oxygen level of the weld deposit decreased, the volume of inclusions also decreased. It is known that to increase Charpy energy especially at temperatures near the upper shelf, the volume on non-metallic incluions should be lowered.[63,64] This relationship is seen to be true for weld deposits.

If the volume of inclusions is reduced, than the dimple size found on a ductile fracture surface should be larger due to the smaller number of inclusions available to initiate microvoid coalesence.[63,64] Figure 37 shows scanning electron micrographs from broken Charpy specimens (+52 C) of the high and low oxygen weld deposits. The dimple size is larger for the lower oxygen weld and indicates a higher energy absorption.

The literature shows that as oxygen is decreased the microstructure tends to have a lower percentage of ferrite veining. This trend is reversed, however, at an oxygen level of about 0.03% where the microstructure becomes less acicular and coarser.[7,65-68] The same trend (although weak) of increasing the amount of acicular ferrite as oxygen level

decreases was found for the flux series of welds. Figure 38 shows the microstructures of the high and low oxygen welds with their respective percent of ferrite veining and oxygen contents. The lower oxygen weld metal is seen to contain less ferrite veining than the higher oxygen weld. It has been suggested that this relationship between microstructure and oxygen is due to the volume of non-metallic inclusions.[62,69,70] The inclusions are felt to enhance transformation at the prior austenite grain boundaries and favor proeutectoid ferrite formation over acicular ferrite which transforms at a slightly later time and also intragranularly.

The inclusions contained in the weld deposits were examined in the electron microprobe using wavelength dispersive x-ray scans on polished surfaces and also in the scanning electron microscope using energy dispersive x-ray analysis on fracture surfaces. The results, although qualitative, show that the inclusions are comprised of titanium, manganese, silicon, aluminum, and oxygen. Figure 39 shows the spectral display of a particle on the fracture surface of a broken Charpy specimen obtained from the energy dispersive system on the scanning electron microscope.

Effects of Electrode Variation

As mentioned in the introduction, molybdenum and nickel can be used to control the microstructure of a weld deposit. Electrode 128 adds molybdenum to the weld deposit and electrode

130 adds molybdenum plus nickel to the deposit. The resulting chemistries are given in Table 11 for the various plates welded with the different wires. Data on Table 12 show that as these two elements are added, the toughness is improved.

The improvement is attributed to the increased hardenability supplied by molybdenum and nickel thereby suppressing the formation of ferrite veining, replacing it with acicular ferrite. Figure 40 shows that as molybdenum is added the amount of ferrite veining is reduced. This effect is consistant with the findings of Yoshino and Stout,[2] Dolby,[41] and Takahashi.[42] Note that the decrease in veining is sufficient to over ride the increase in hardness and strength. It also improves the toughness. An analogous effect is the improved toughness and increased hardness and strength obtained with grain refinement. In the present situation, a coarse "grain" structure (ferrite veining) is replaced by a finer "grain" structure (acicular ferrite).

The effect of these two elements is active at both high and low titanium levels as evidenced by welds T107 and S062. However, the deleterious effect of titanium is also active in the presence of molybdenum as seen in comparing welds S062 and W059. Weld S062 (high titanium) has lower toughness than weld W059 (no titanium) when both are welded with the molybdenum containing electrode.

SUMMARY AND CONCLUSIONS

The findings of this study demonstrate that although titanium is detrimental to the toughness of submerged-arc welds on HSLA steels, its deleterious effects can be offset by proper selection of welding consumables. Specifically, this study shows:

1. Toughness is strongly dependent on the titanium and manganese levels. The toughness increases with decreasing titanium and increasing manganese. Titanium increases the maximum weld metal hardness through solid solution hardening and also increases the amount of ferrite veining at low manganese levels. Manganese decreases the amount of ferrite veining and refines the microstructure. Carbon and silicon have comparatively weak effects, with carbon decreasing and silicon increasing the toughness.

2. Toughness is improved by using higher basicity fluxes. These fluxes reduce the oxygen level with a concomitant reduction in inclusion volume. Also, ferrite veining is reduced slightly with the higher basicity fluxes.

3. Molybdenum or molybdenum plus nickel additions improve toughness by reducing the amount of ferrite veining.

4. Maximum hardness increases with carbon, manganese, and titanium contents. The effect of silicon is ill-defined.

5. Yield and tensile strengths increase with carbon, manganese, silicon, and titanium content. Manganese and silicon have comparatively weaker effects on yield and tensile strength, respectively.

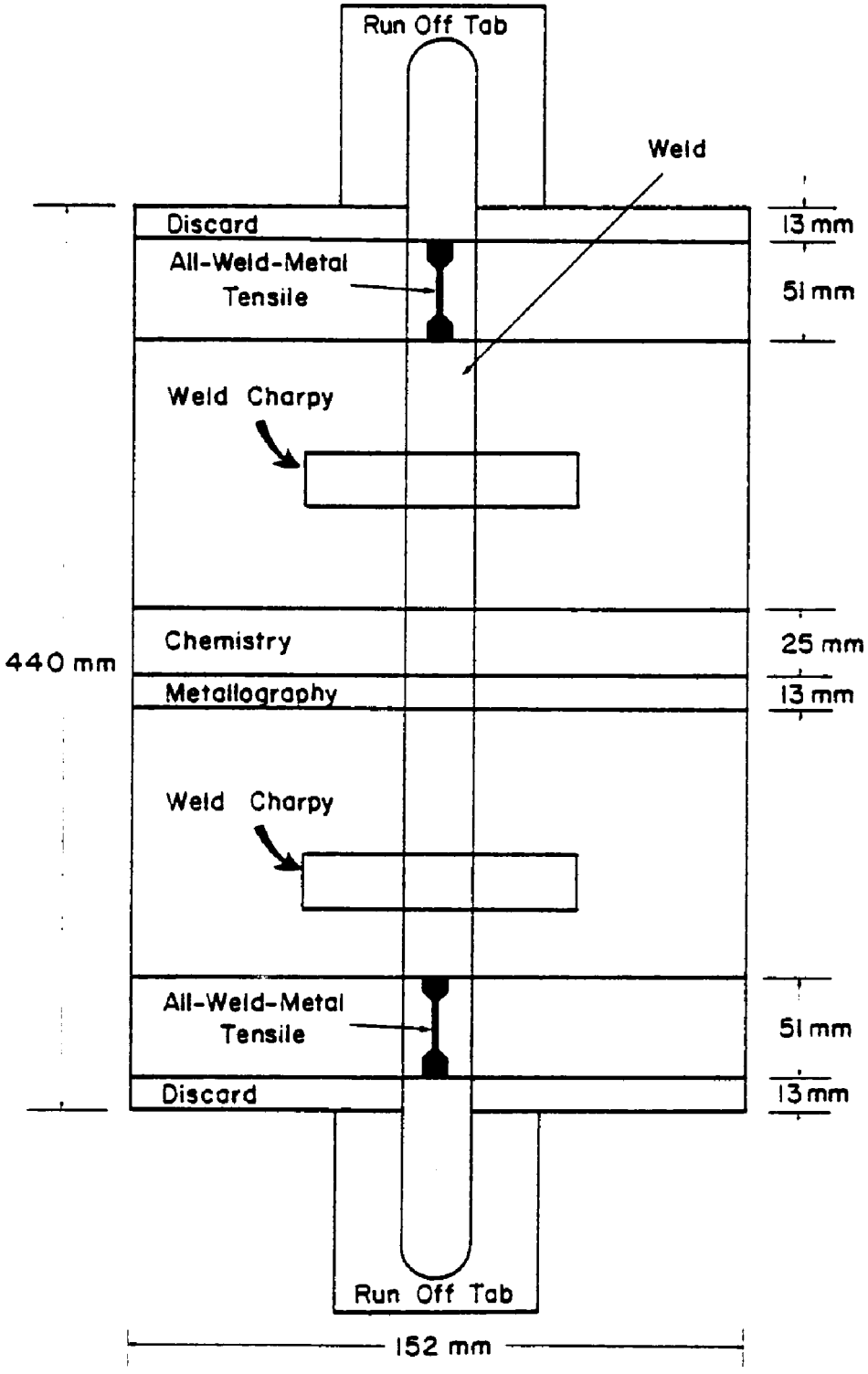

Figure 1. Schematic Diagram of Test Plate and Specimen Location.

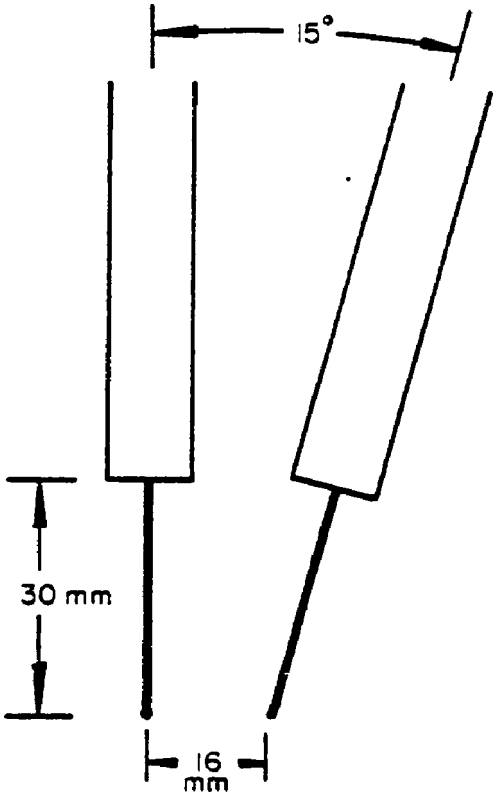

Figure 2. Orientation of the Welding Electrodes.
Travel direction is right to left.

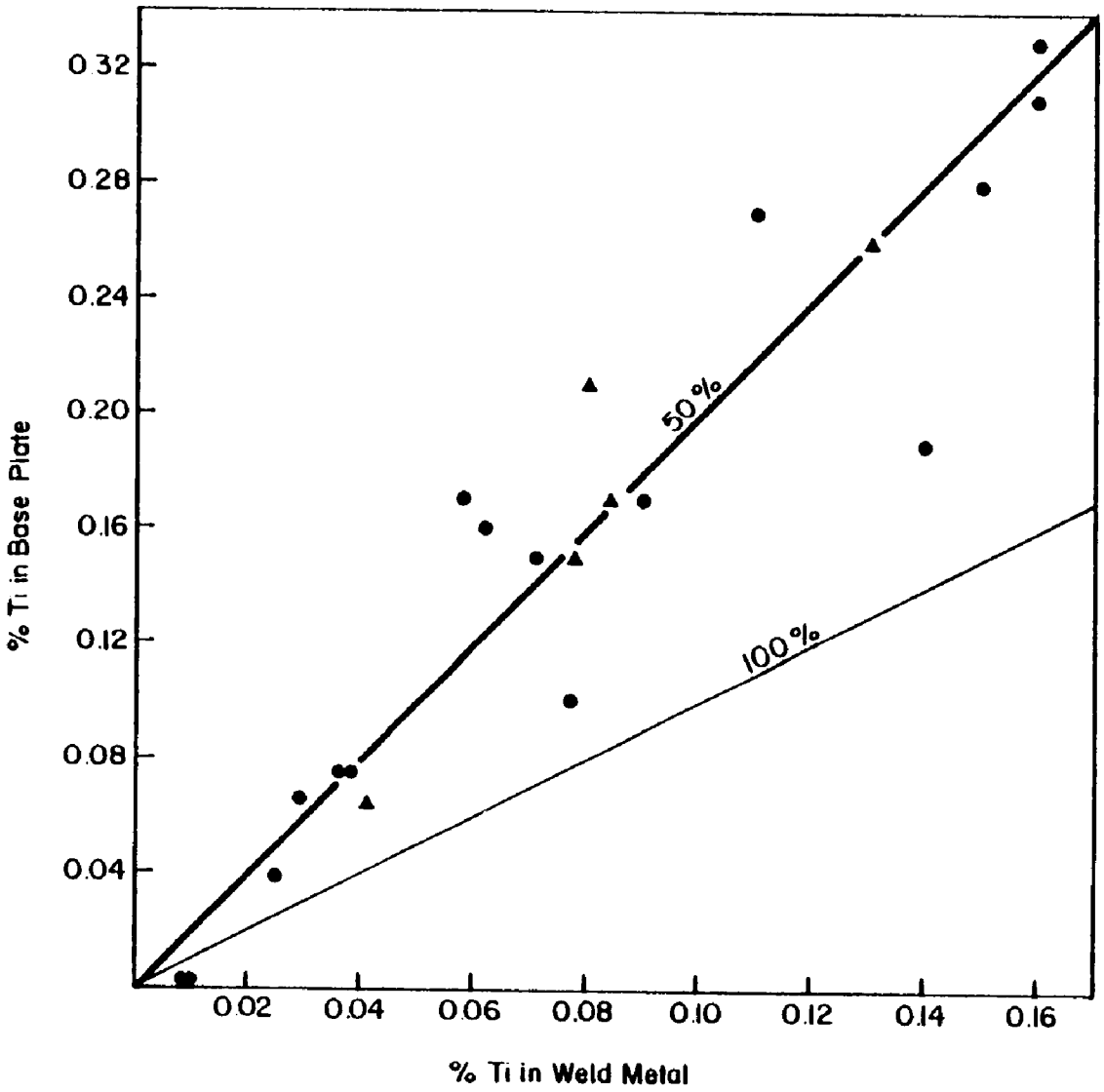

Figure 3. Titanium Dilution
Triangles represent low-manganese welds and circles represent high-manganese welds

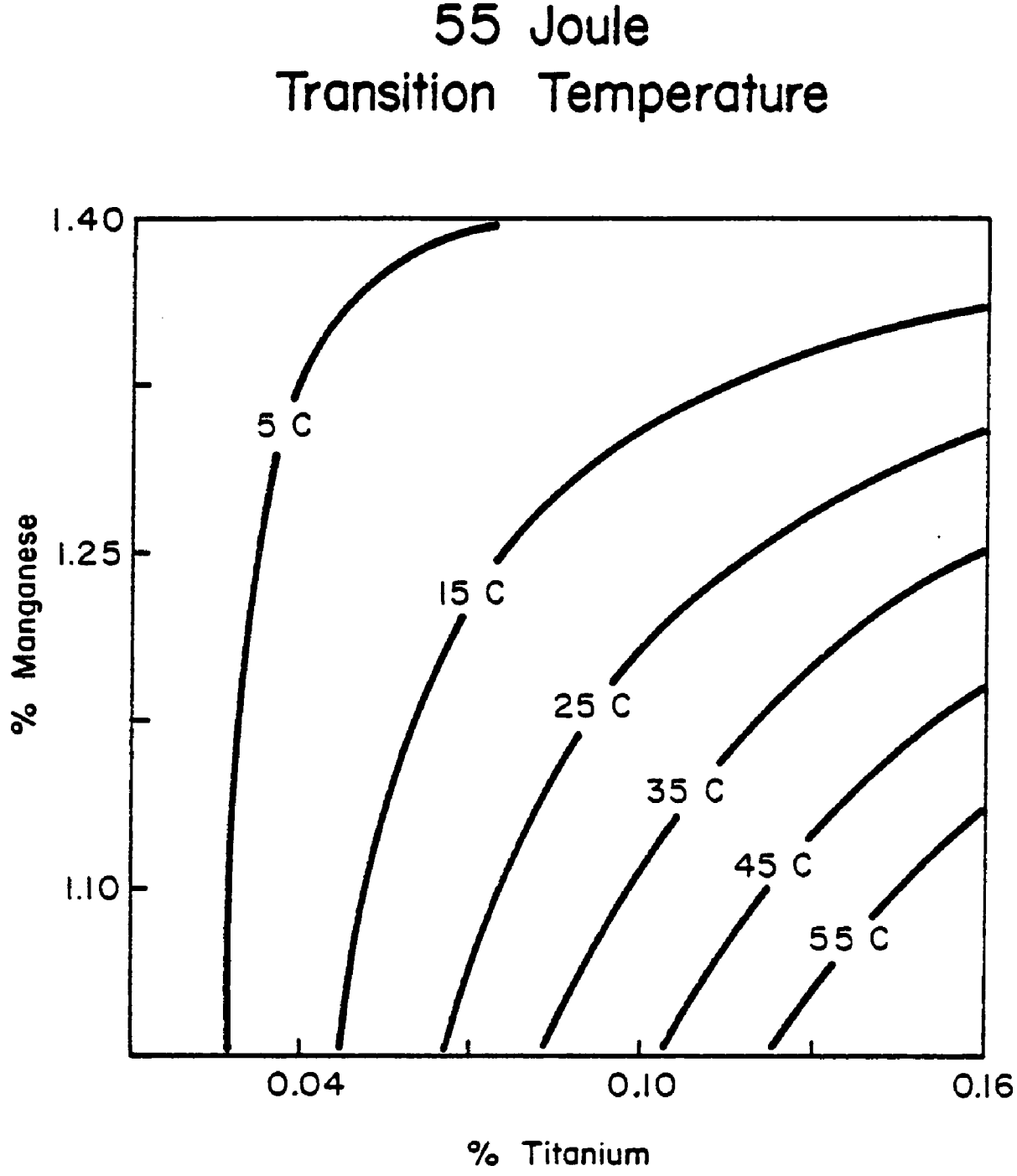

Figure 4. 55 Joule Transition Temperature Versus Titanium and Manganese at 0.09% Carbon; CTM Series.

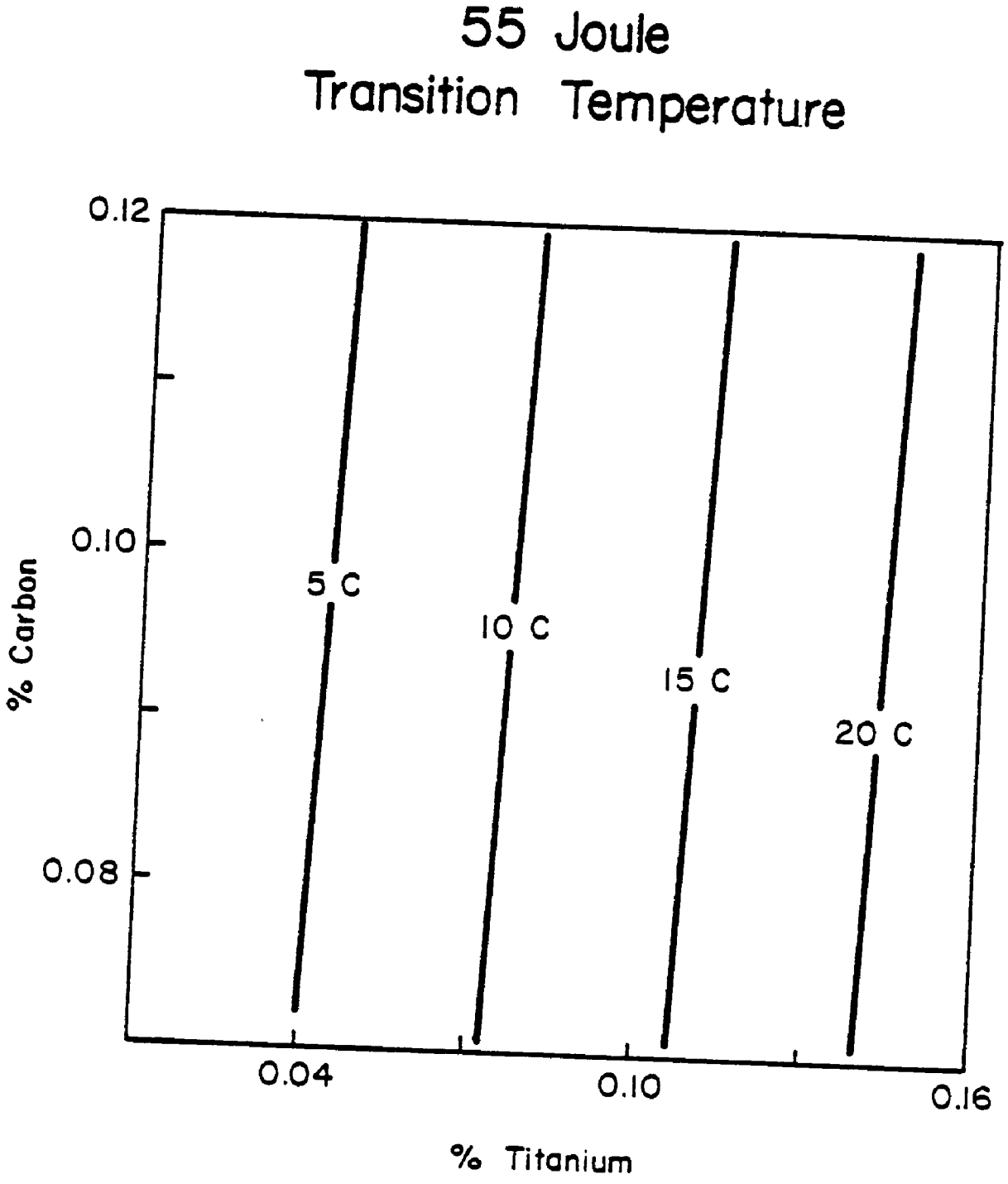

Figure 5. 55 Joule Transition Temperature Versus Titanium and Carbon at 0.475% Silicon; CTS Series.

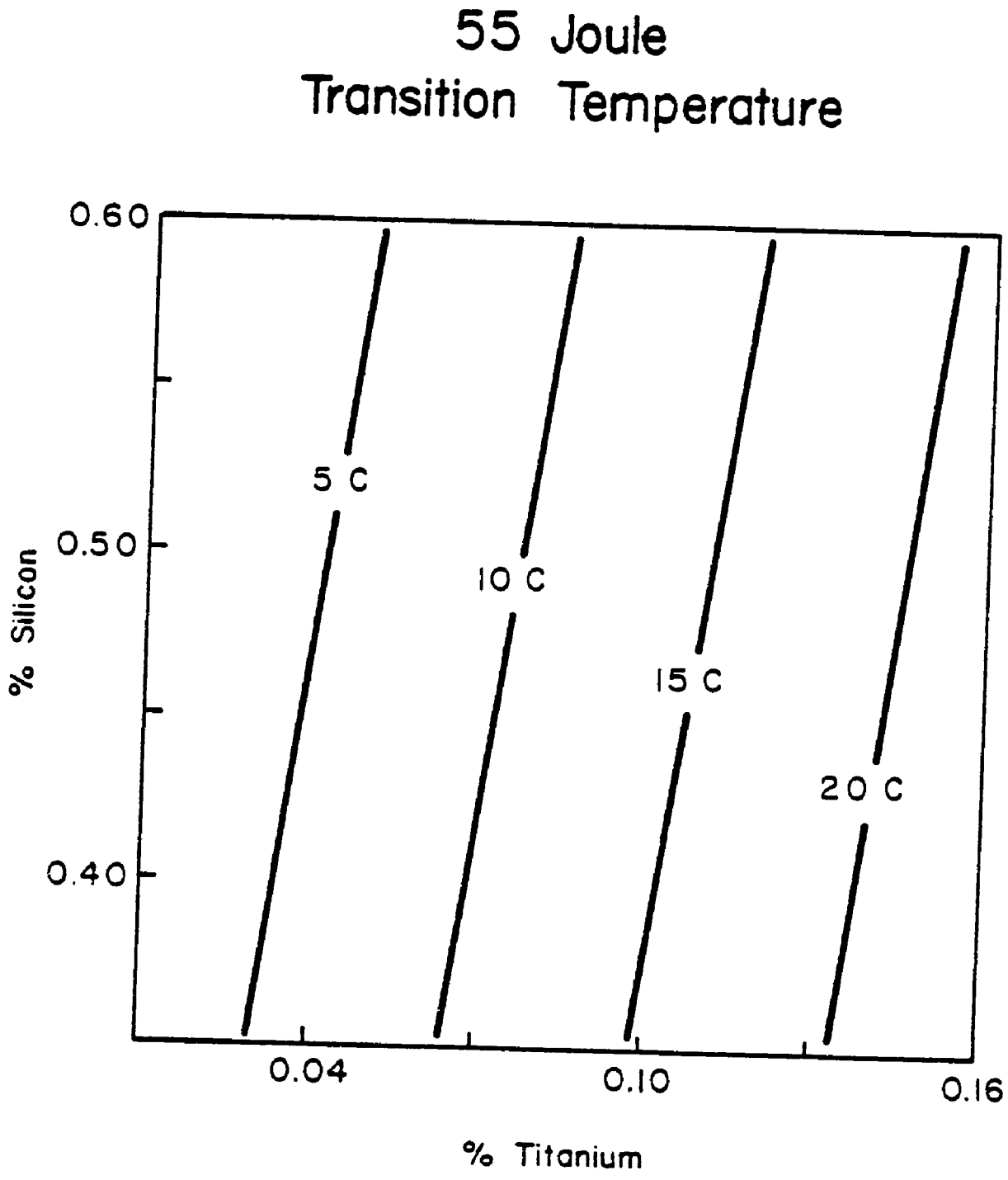

Figure 6. 55 Joule Transition Temperature Versus Titanium and Silicon at 0.09% Carbon: CTS Series.

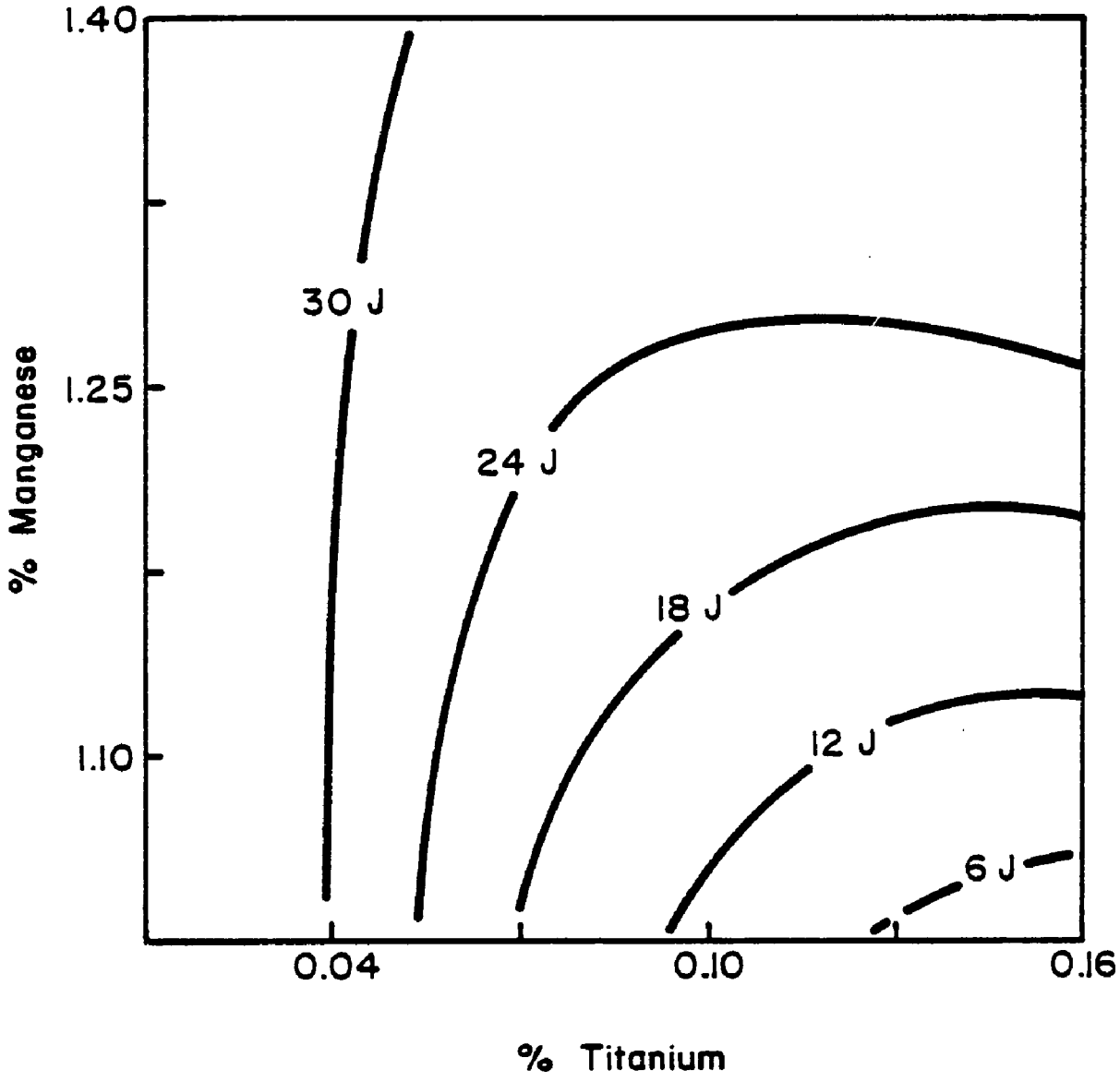

Figure 7. Charpy Energy at -18 C Versus Titanium and Manganese at 0.09% Carbon; CTM Series.

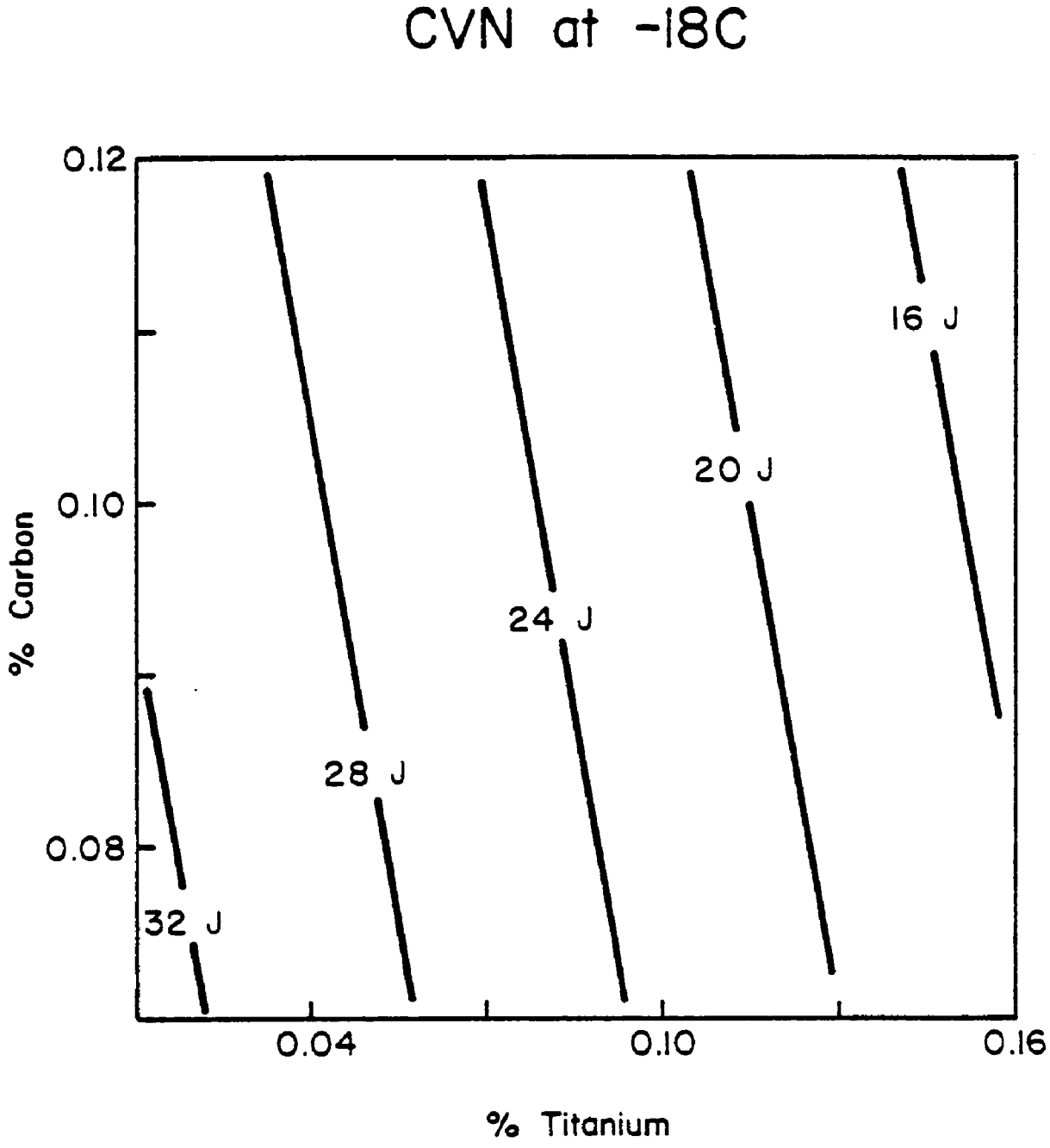

Figure 8. Charpy Energy at -18 C Versus Titanium and Carbon at 0.35% Silicon; CTS Series.

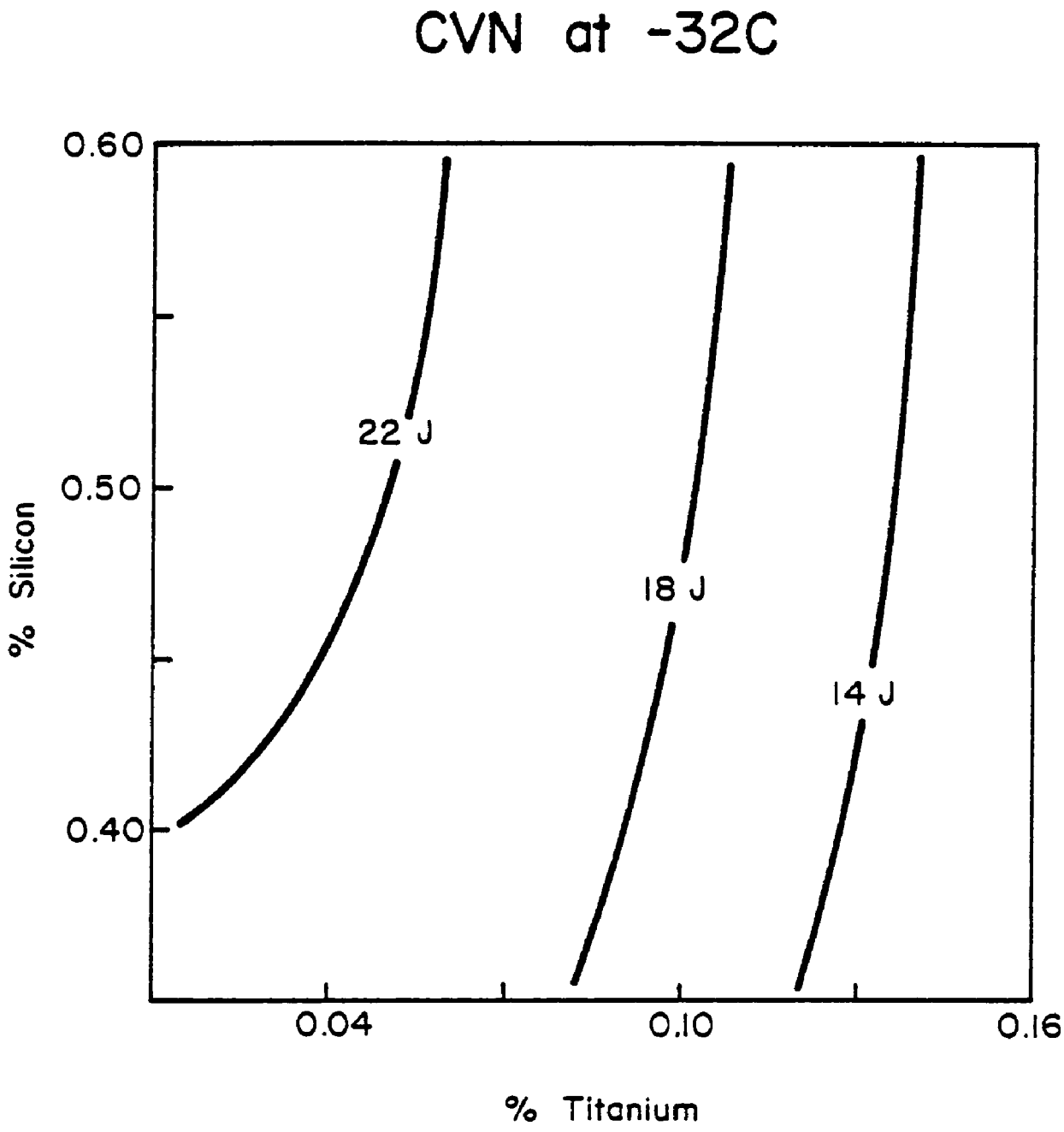

Figure 9. Charpy Energy at -32 C Versus Titanium and Silicon at 0.09% Carbon; CTS Series.

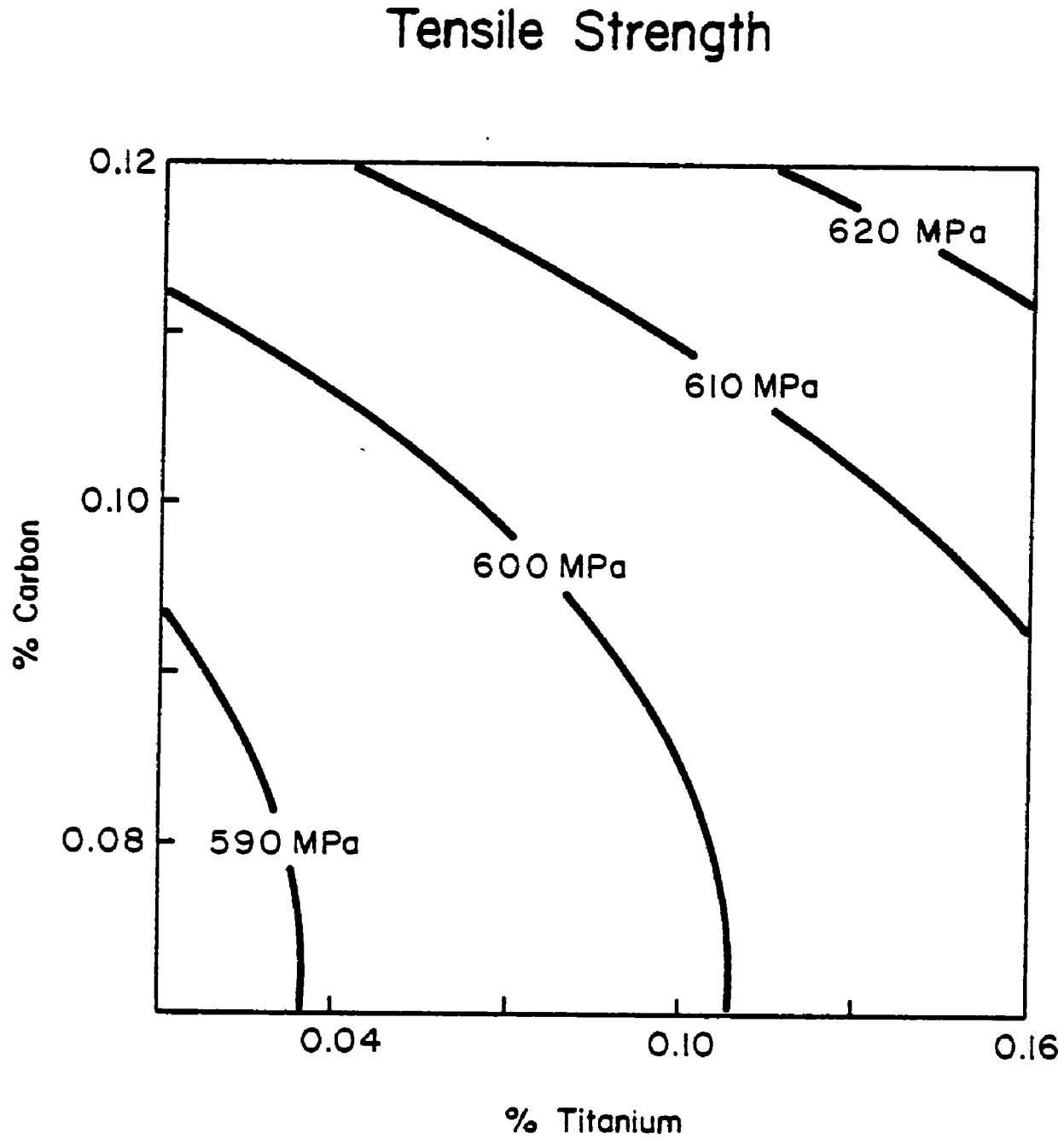

Figure 10. Tensile Strength Versus Titanium and Carbon at 1.20% Manganese; CTM Series.

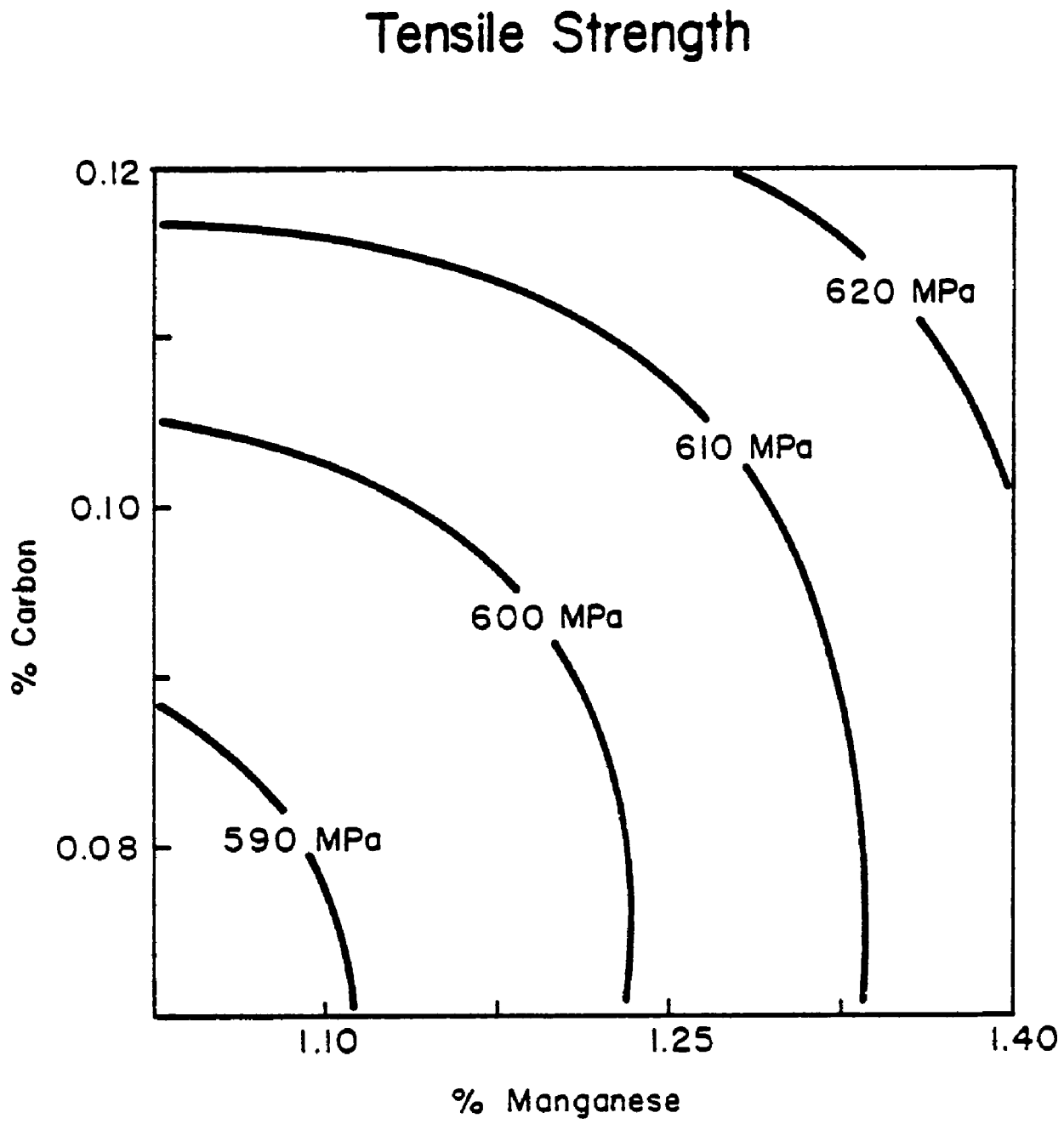

Figure 11. Tensile Strength Versus Manganese and Carbon at 0.085% Titanium; CTM Series.

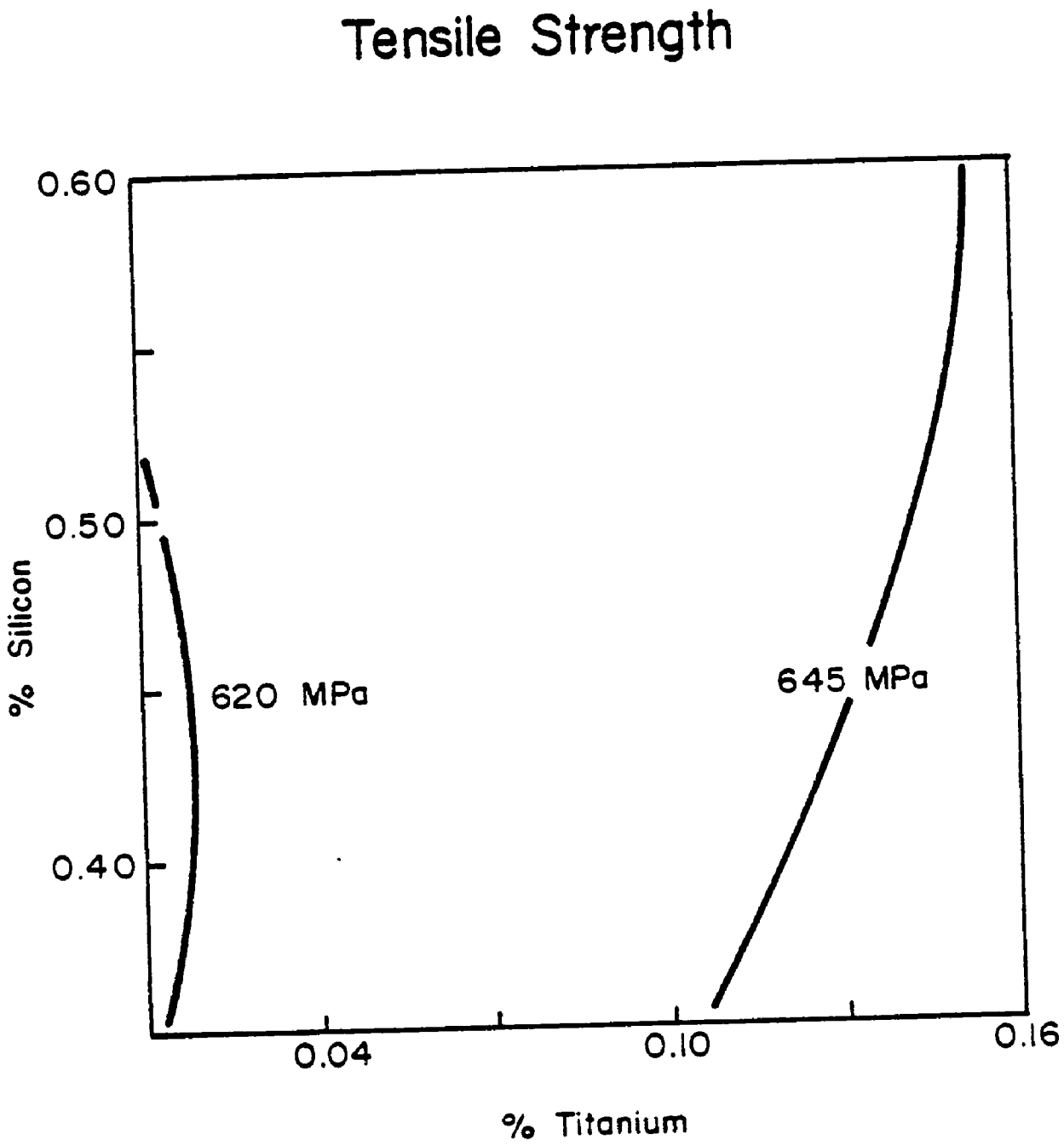

Figure 12. Tensile Strength Versus Titanium and Silicon at 0.12% Carbon; CTS Series.

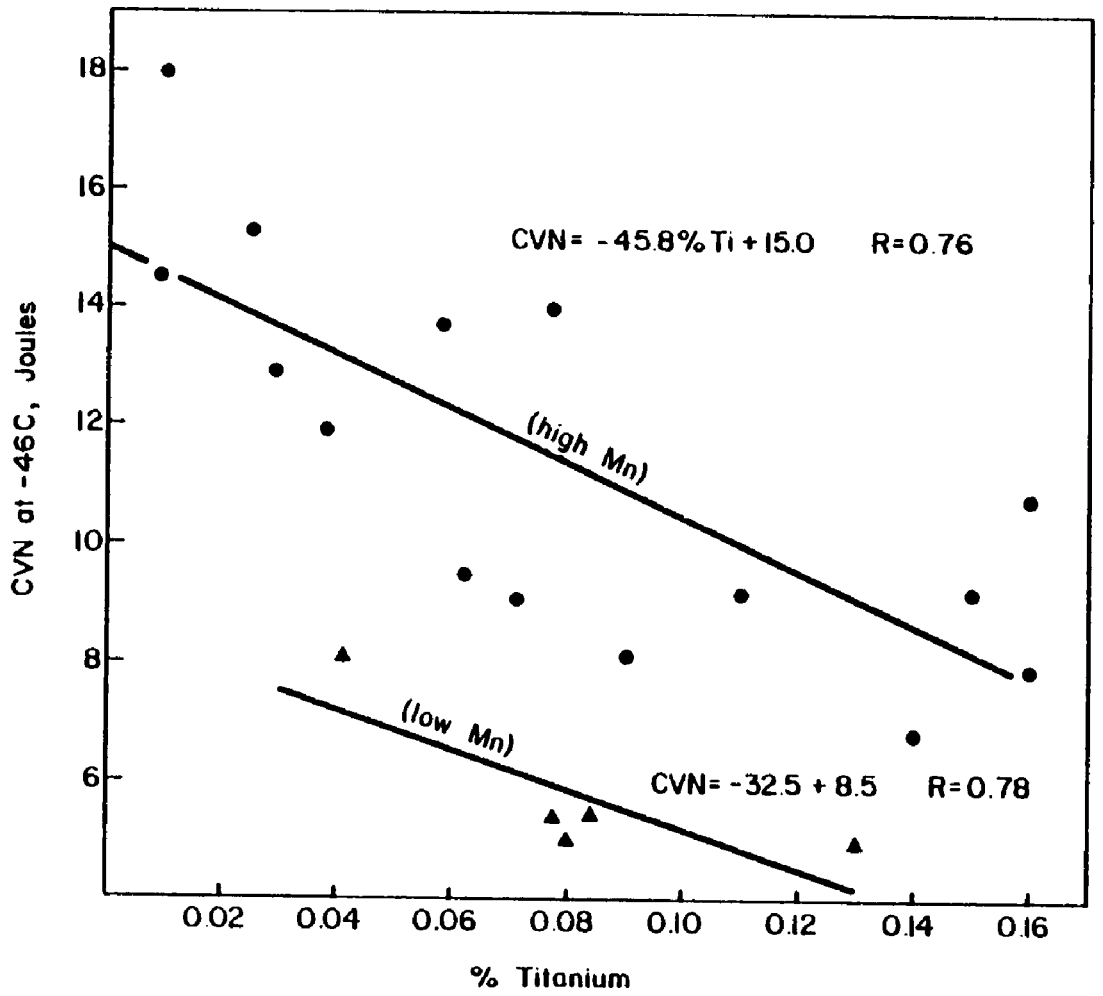

Figure 13. Charpy Energy at -46 C Versus Titanium. High manganese is nominally 1.3% and low manganese is nominally 1.05%. Equations are least squares fit.

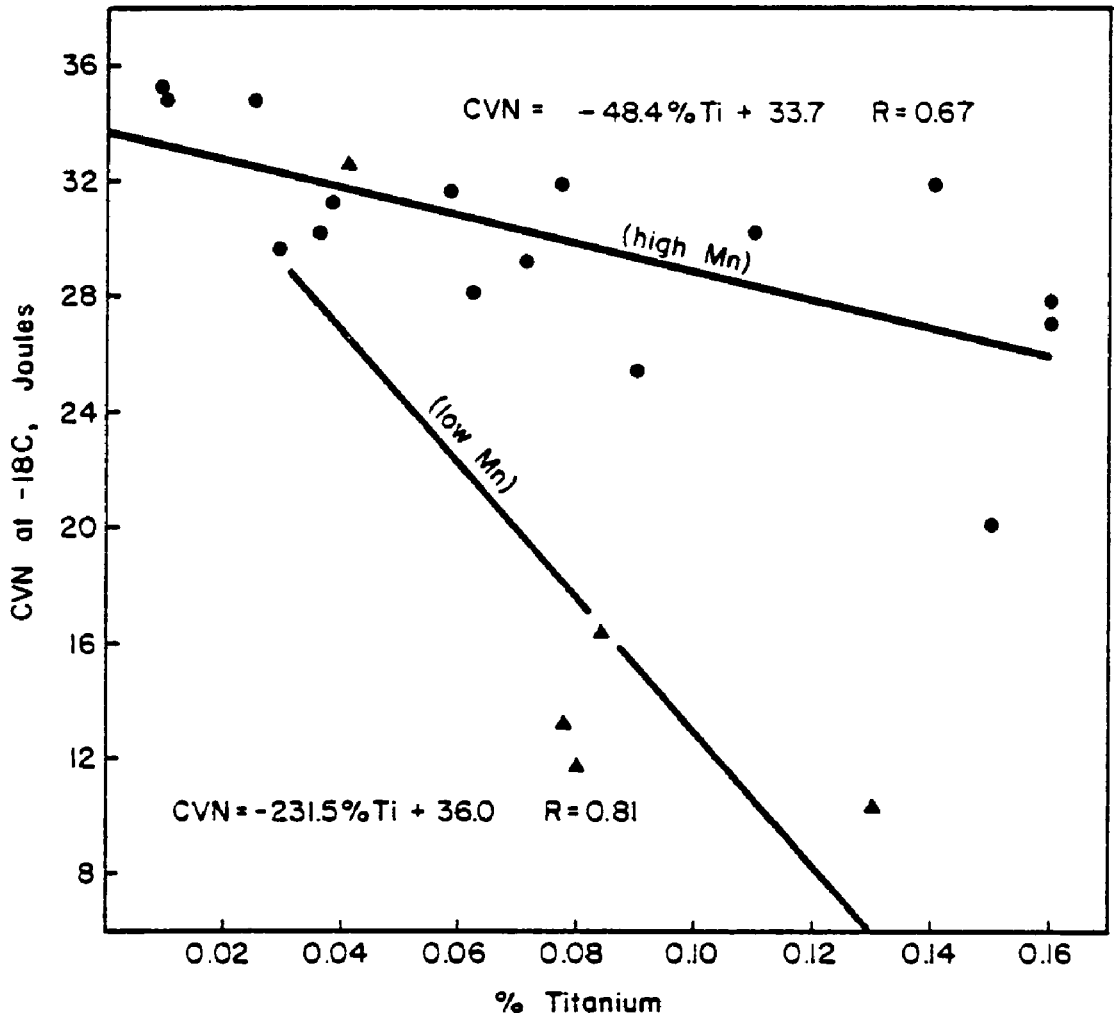

Figure 14. Charpy Energy at -18 C Versus Titanium. High manganese is nominally 1.3% and low manganese is nominally 1.05%. Equations are least squares fit.

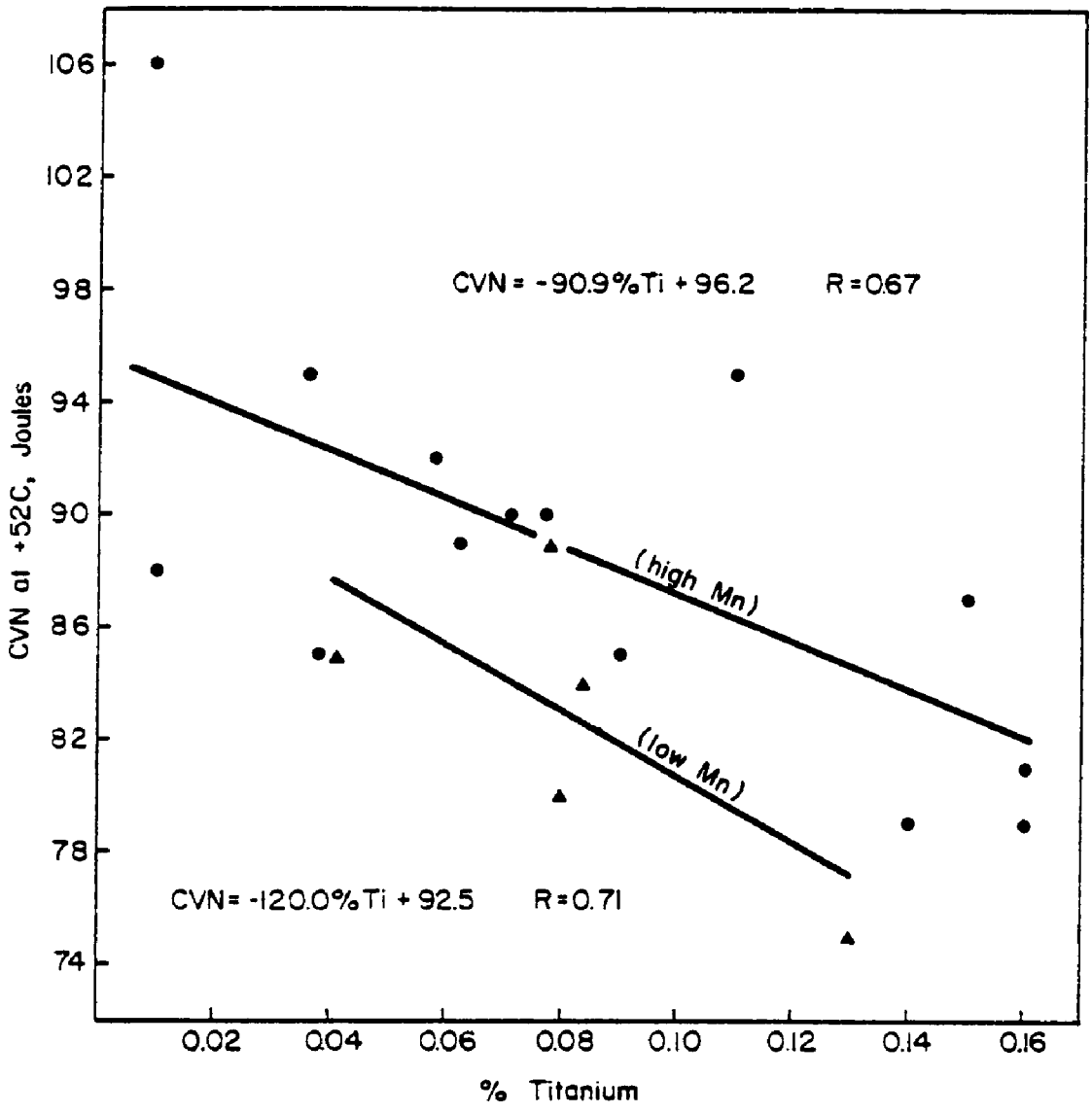

Figure 15. Charpy Energy at +52 C Versus Titanium. High manganese is nominally 1.3% and low manganese is nominally 1.05%. Equations are least squares fit.

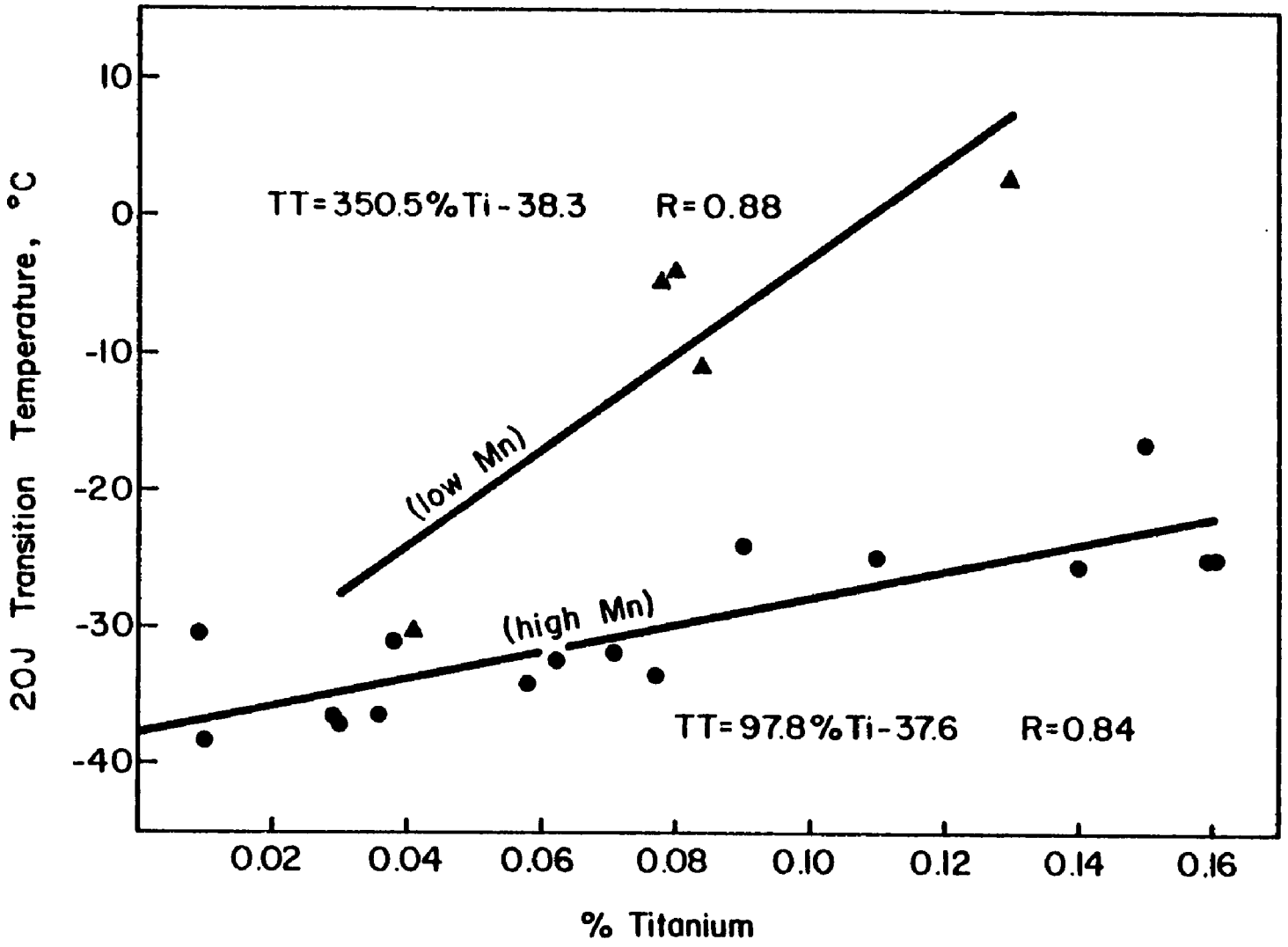

Figure 16. 20 Joule Transition Temperature Versus Titanium.

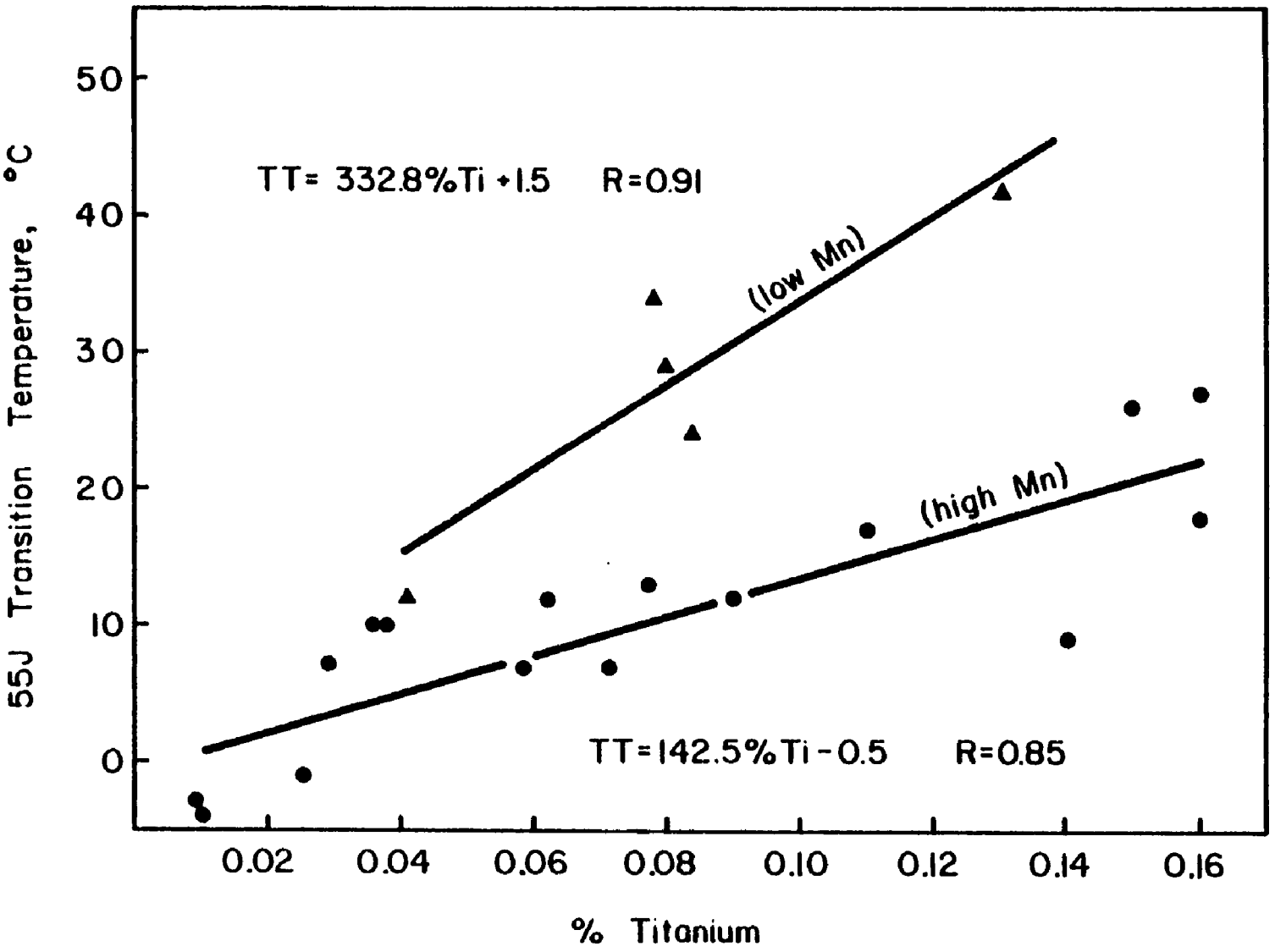

Figure 17. 55 Joule Transition Temperature Versus Titanium.

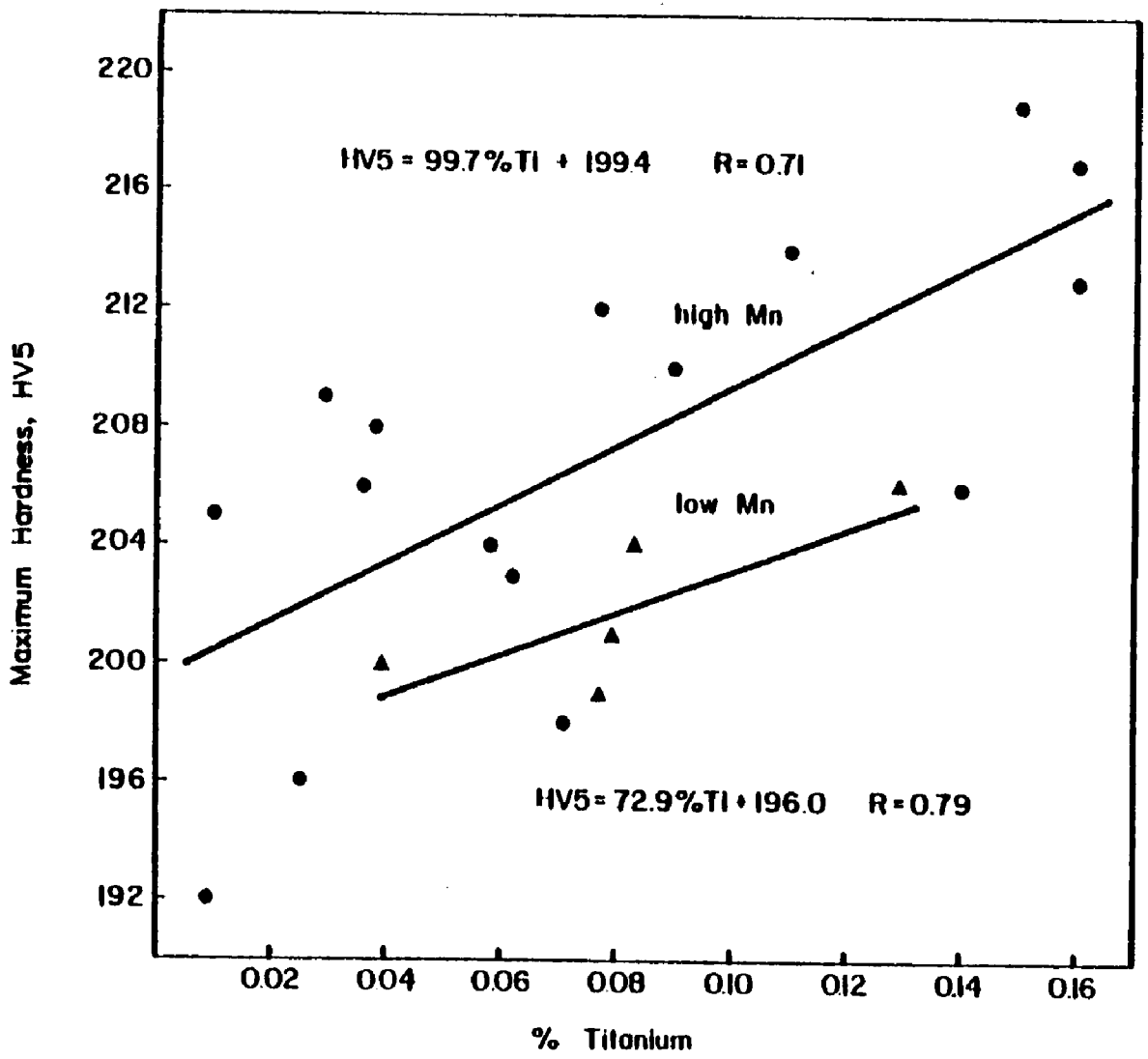

Figure 18. Maximum Hardness Versus Titanium.

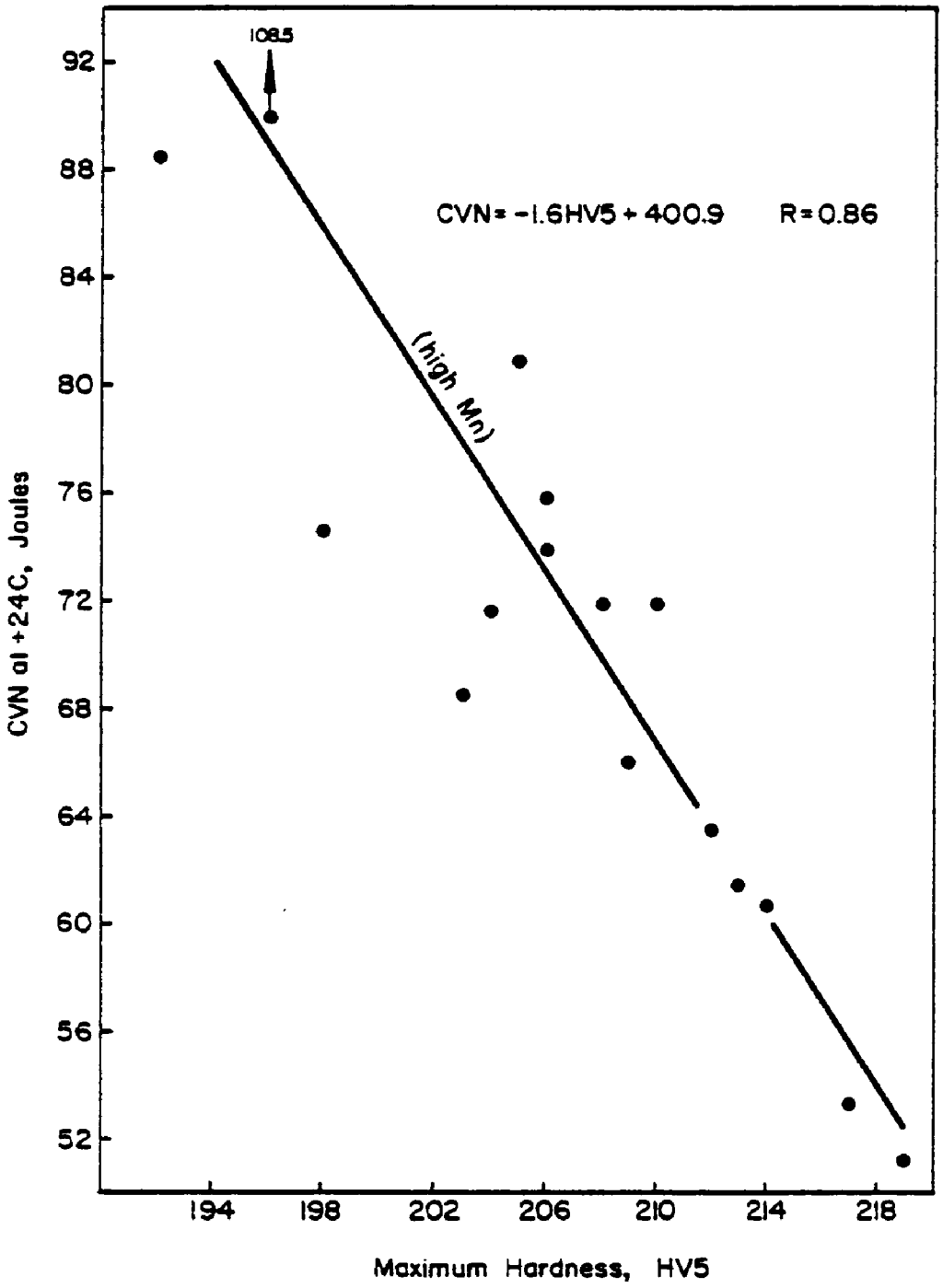

Figure 19. Charpy Energy at +24 C Versus Maximum Hardness. Manganese is nominally 1.3%. Equation is least squares fit.

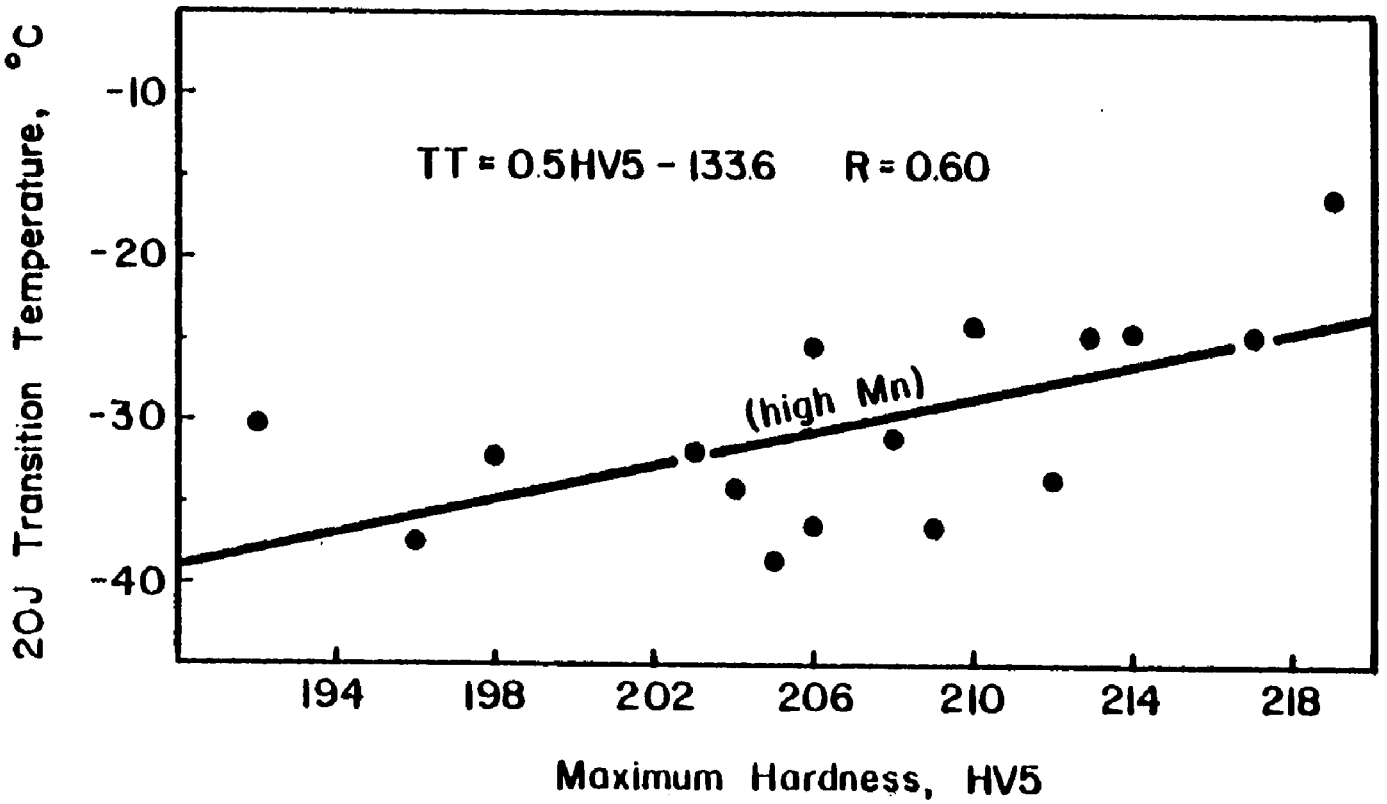

Figure 20. 20 Joule Transition Temperature Versus Maximum Hardness. Manganese is nominally 1.3%. Equation is least squares fit.

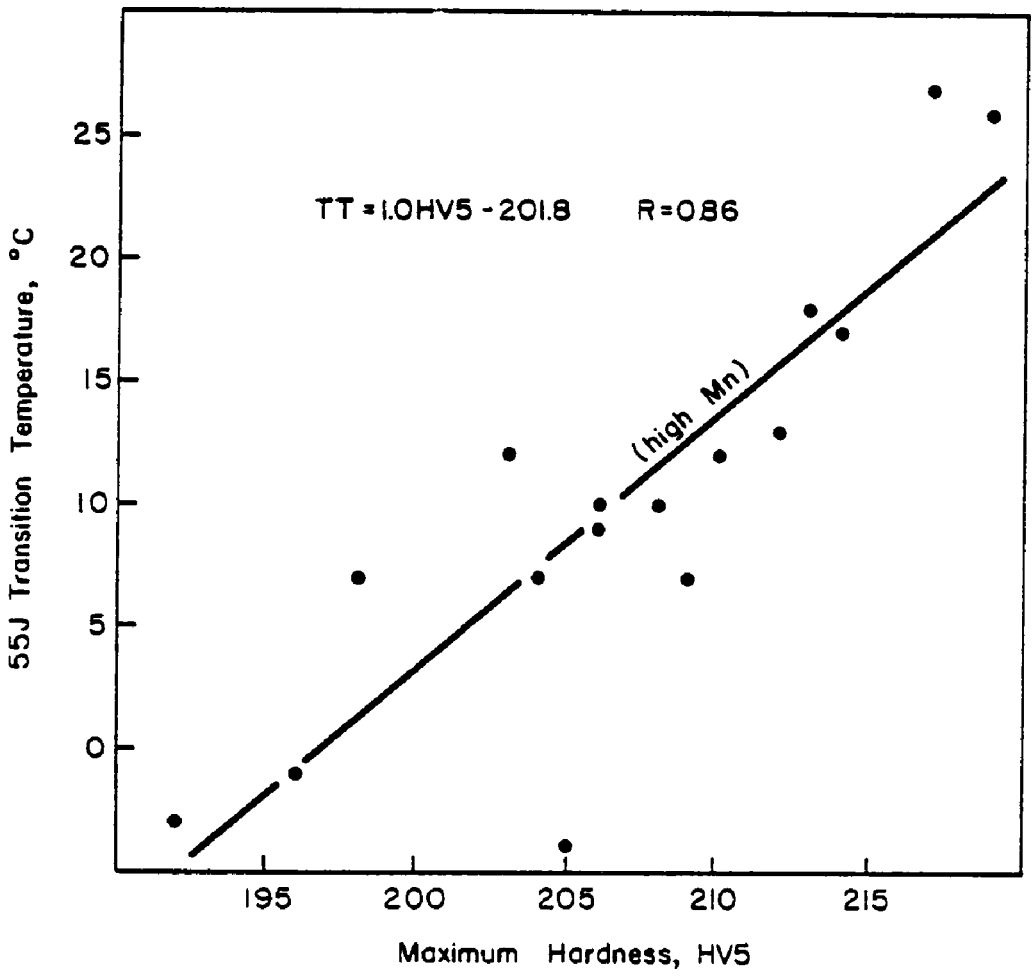

Figure 21. 55 Joule Transition Temperature Versus Maximum Hardness. Manganese is nominally 1.3%. Equation is least squares fit.

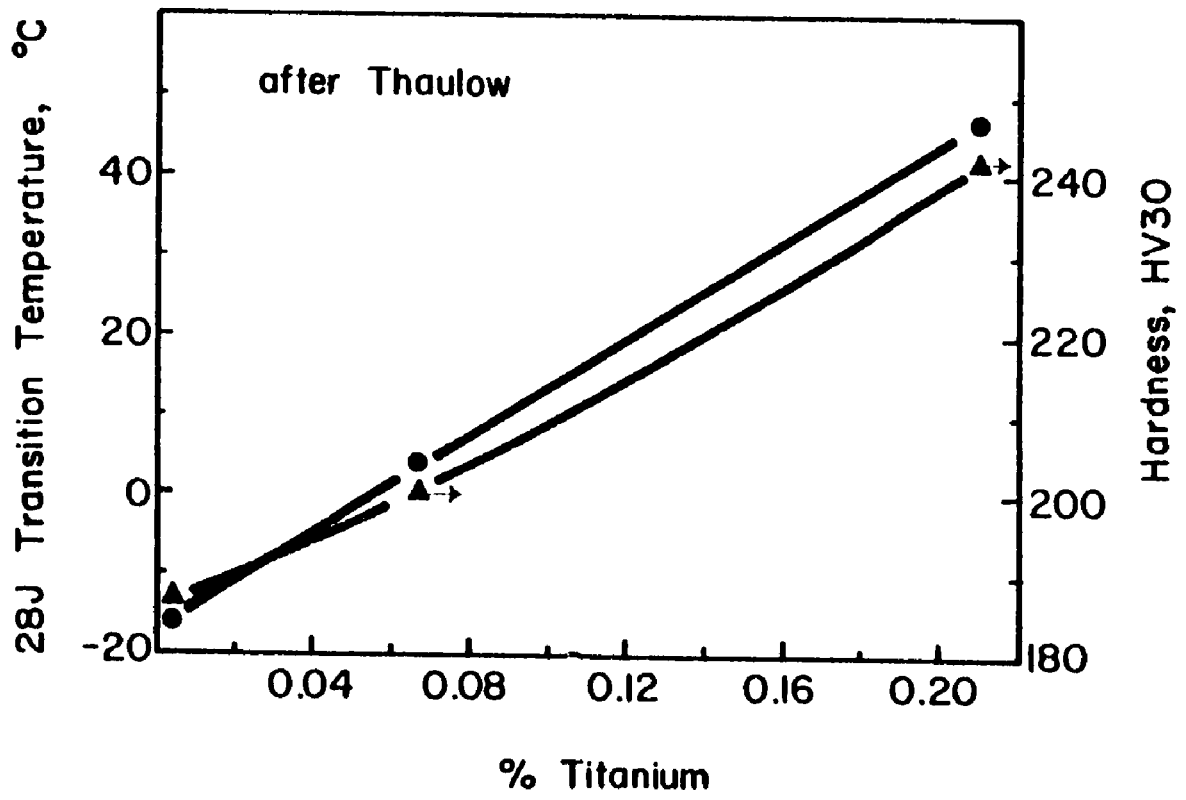

Figure 22. 28 Joule Transition Temperature Versus Hardness and Titanium

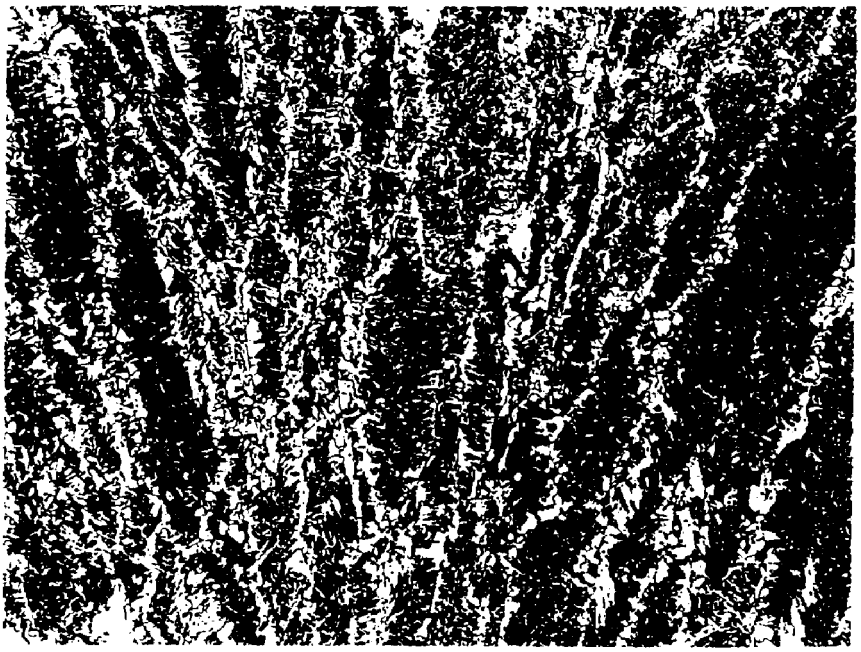

23A Ferrite Veining Nital 100X Weld S060

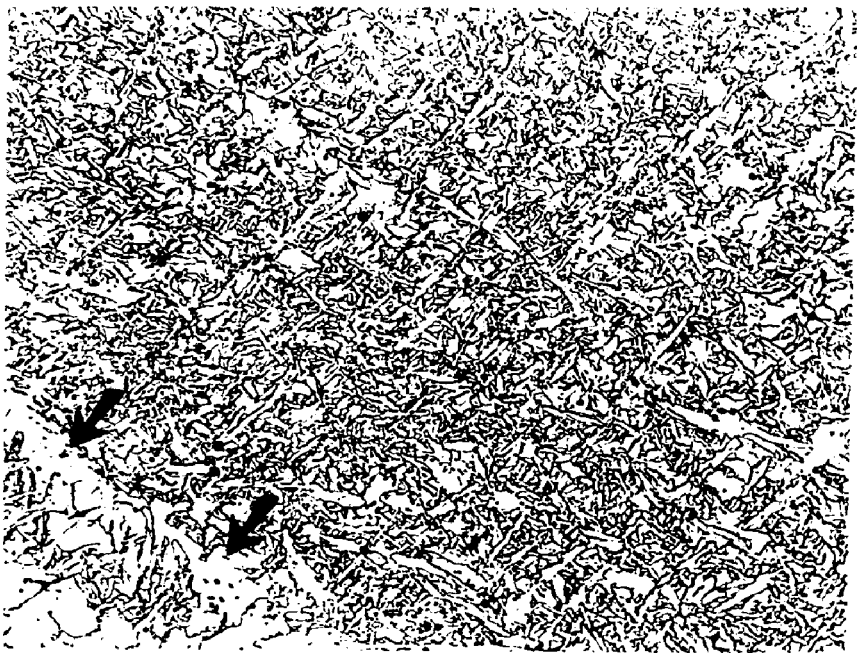

23B Acicular Ferrite Nital 500X Weld S060

Figure 23. Microconstituents in a HSLA Steel Weld Deposit.

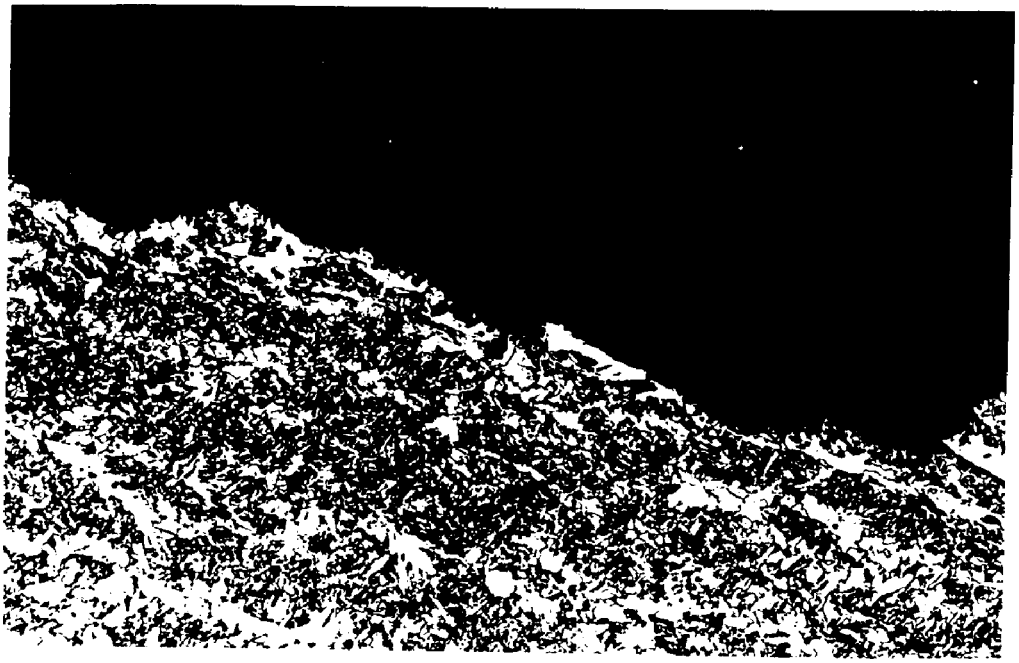

Figure 24. Crack Propagation Path Through Ferrite Veins.

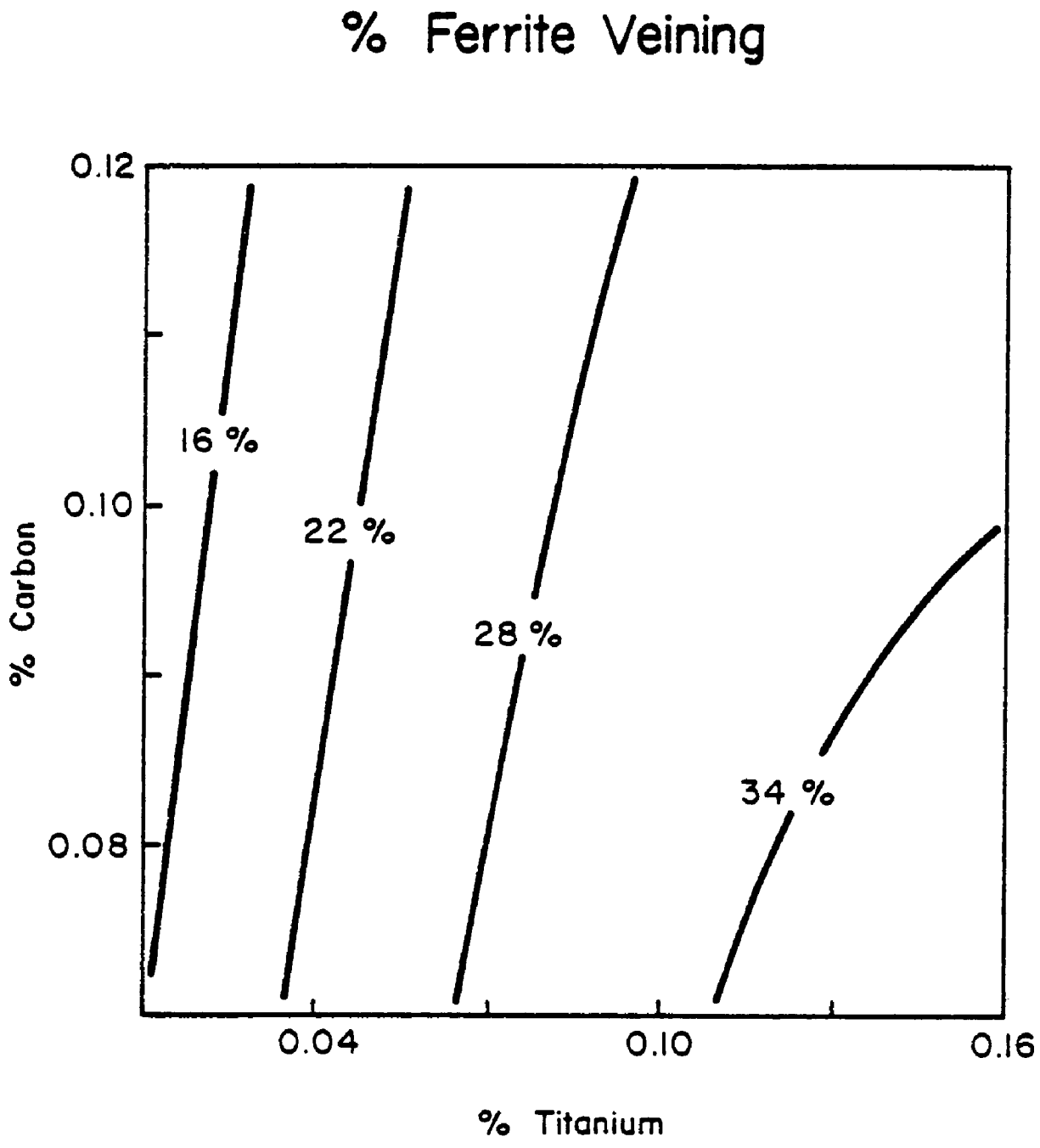

Figure 25. % Ferrite Veining Versus Titanium and Carbon at 1.05% Manganese; CTM Series.

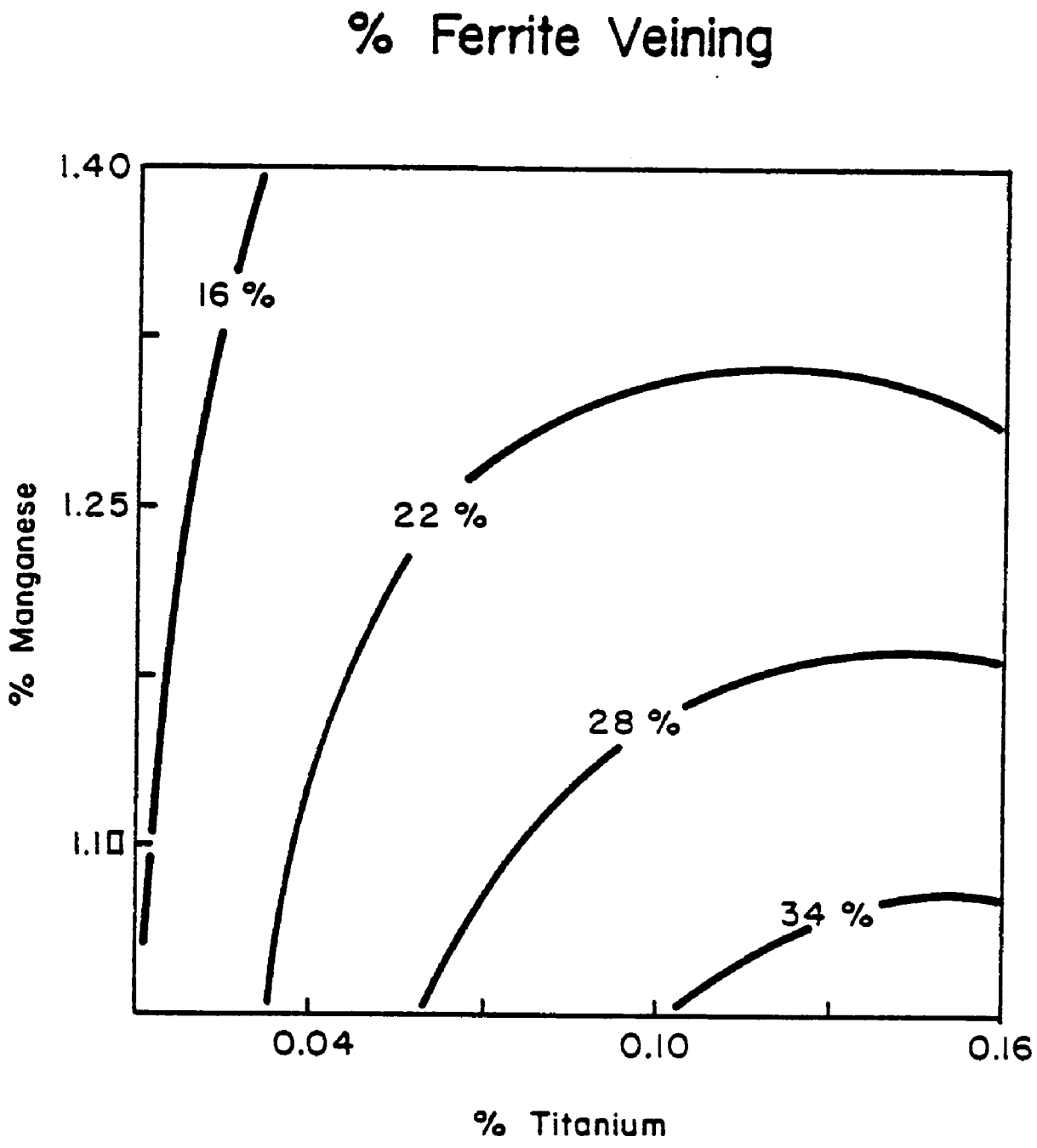

Figure 26. % Ferrite Veining Versus Titanium and Manganese at 0.07% Carbon; CTM Series.

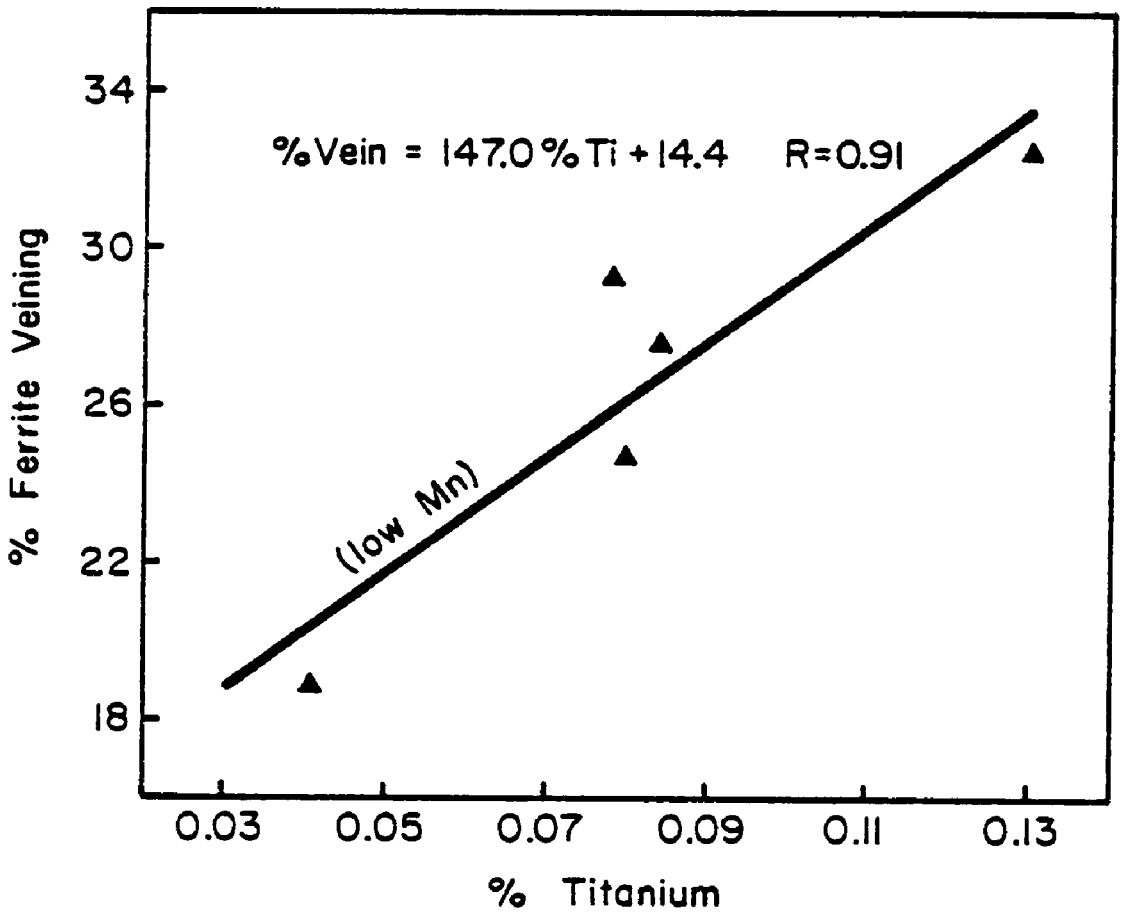

Figure 27. % Ferrite Veining Versus Titanium. Manganese is nominally 1.05%. Equation is least squares fit.

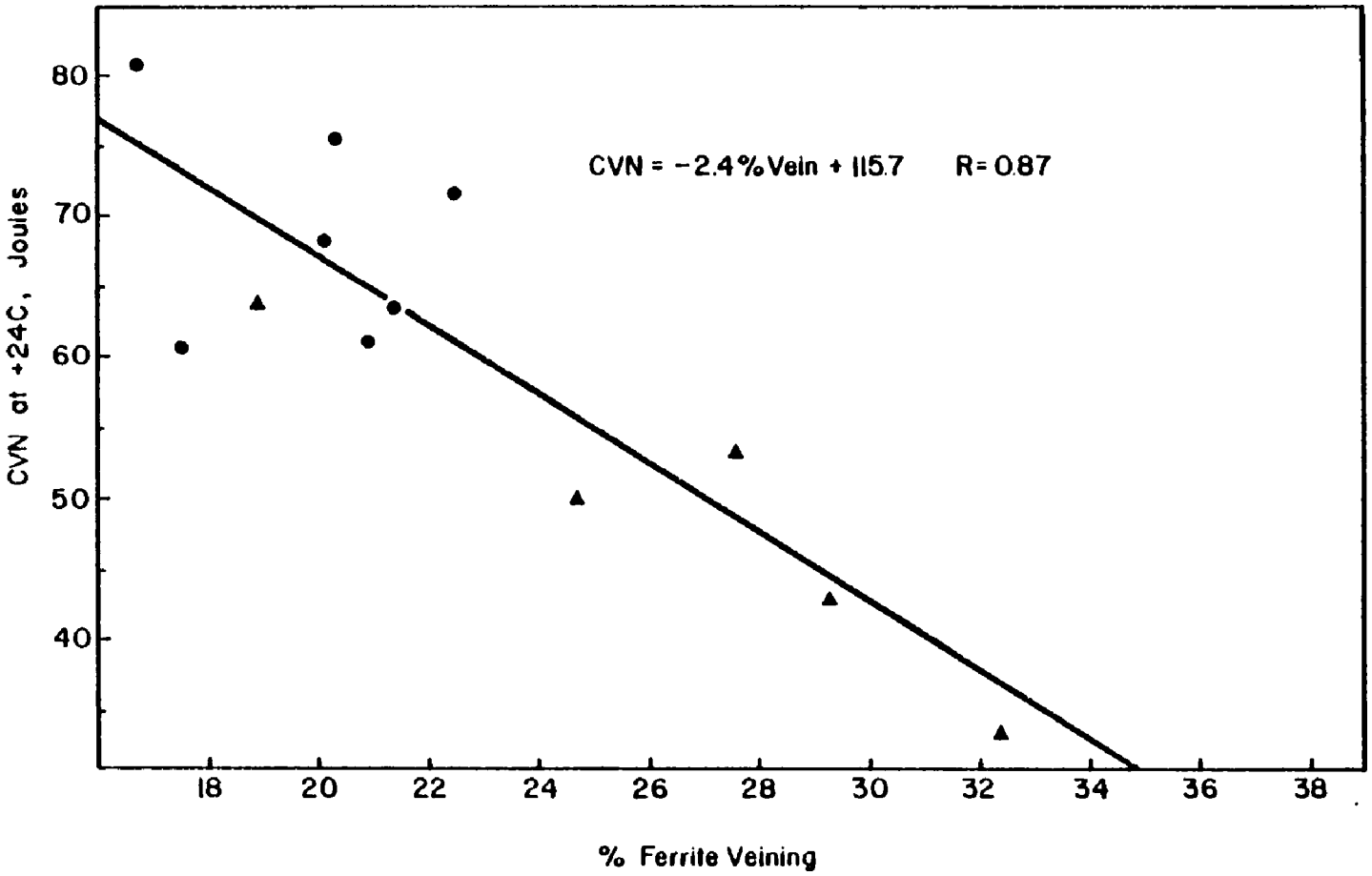

Figure 28. Charpy Energy at +24 C Versus % Ferrite Veining. CTM Series. Equation is least squares fit.

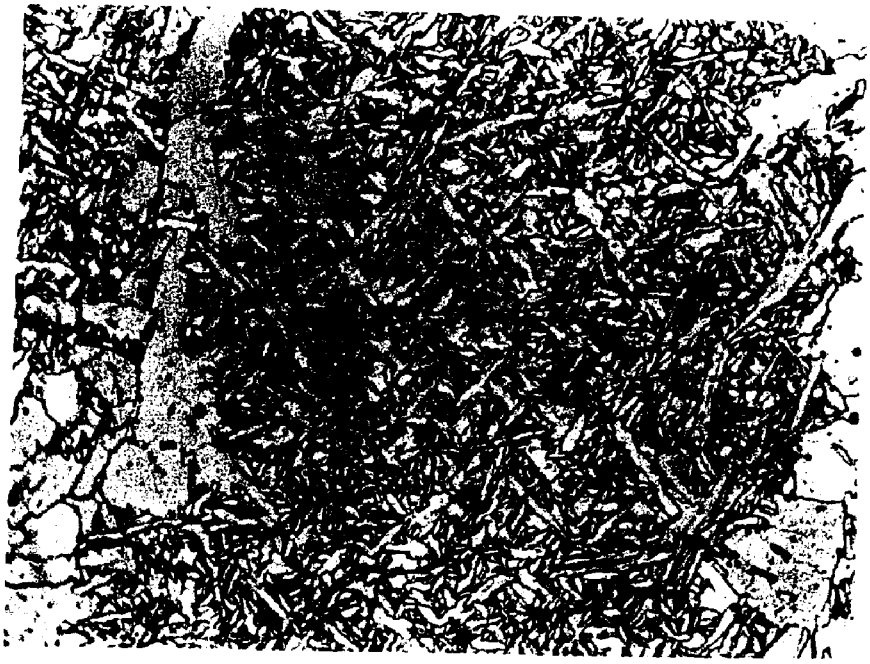

29A As-Cast Structure Nital 500X Weld W058

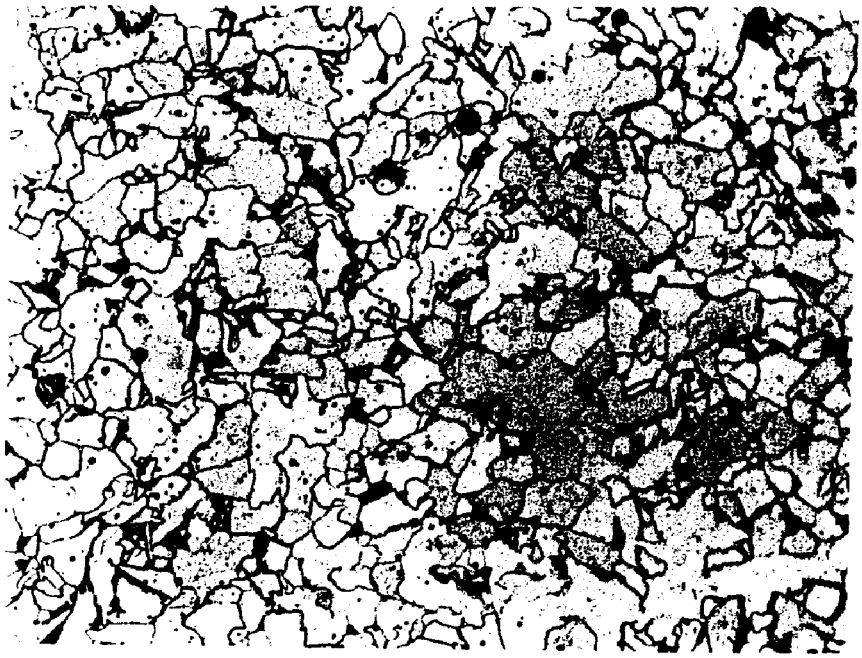

29B Reheated Structure Nital 500X Weld W058

Figure 29. As-Cast and Reheated Microstructures in a HSLA Steel Weld Deposit.

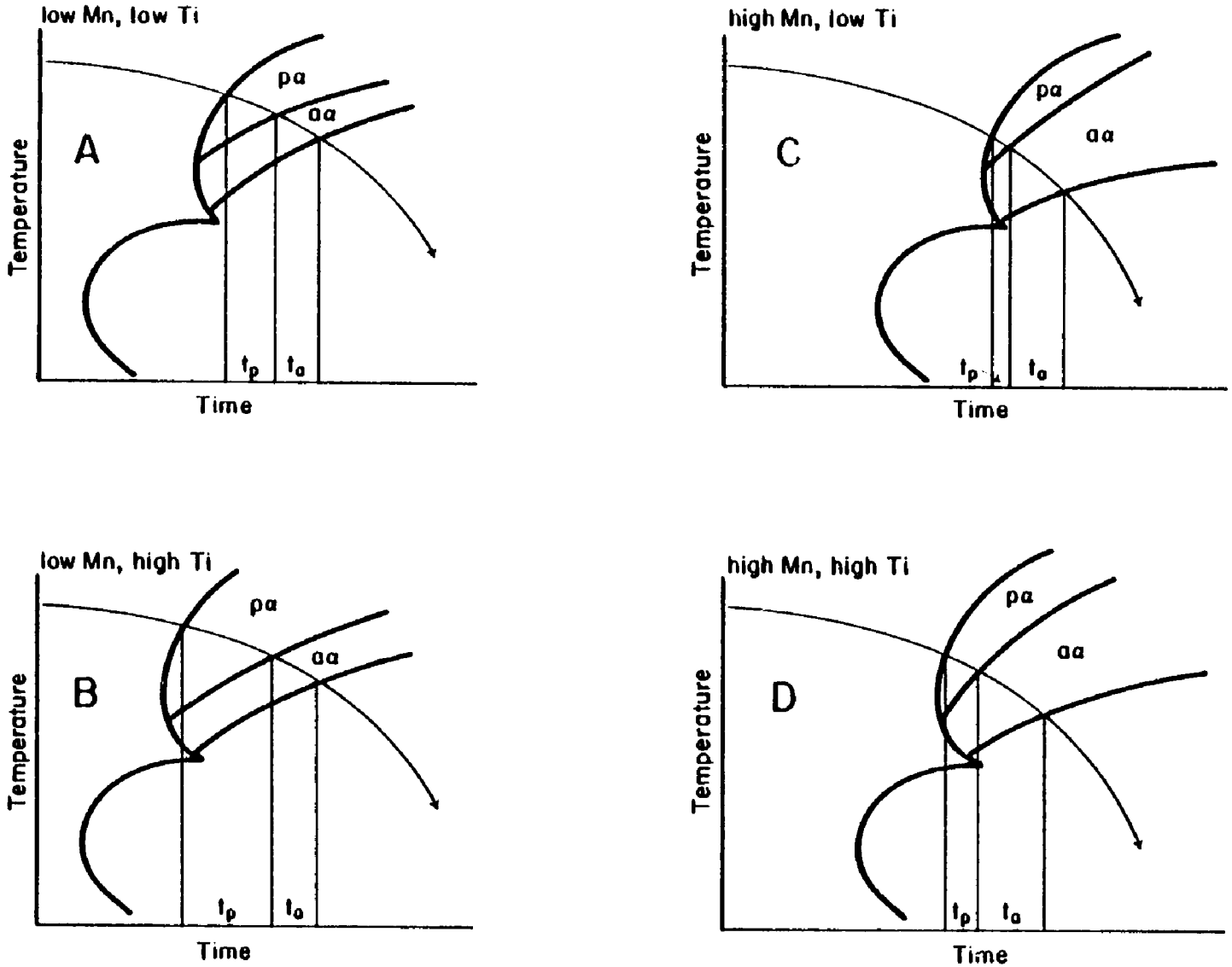

Figure 30. Hypothetical Continuous Cooling Diagrams Derived from Post-Solidification Cooling.

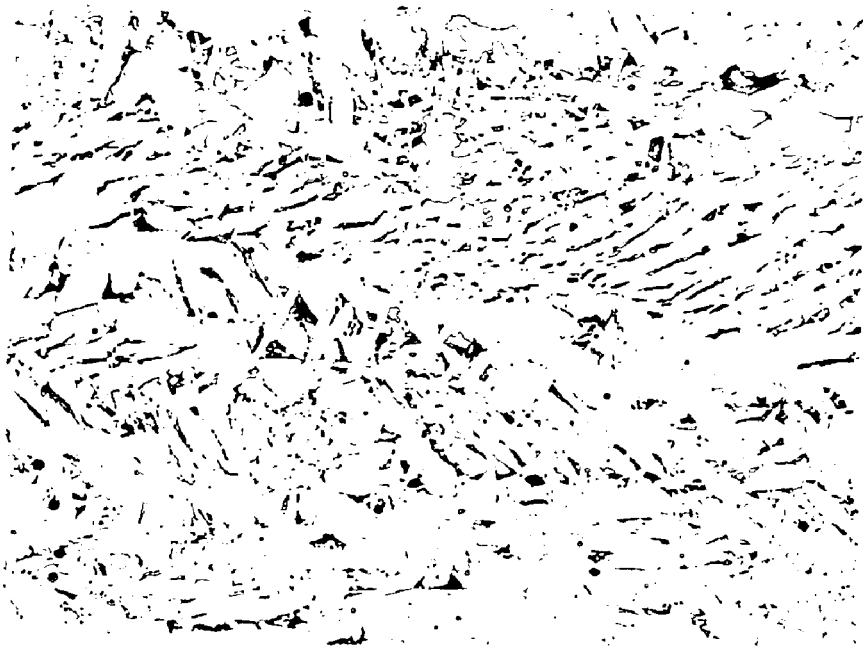

31A 1.07% Mn 10J @ -18 C Nital 500X Weld S068

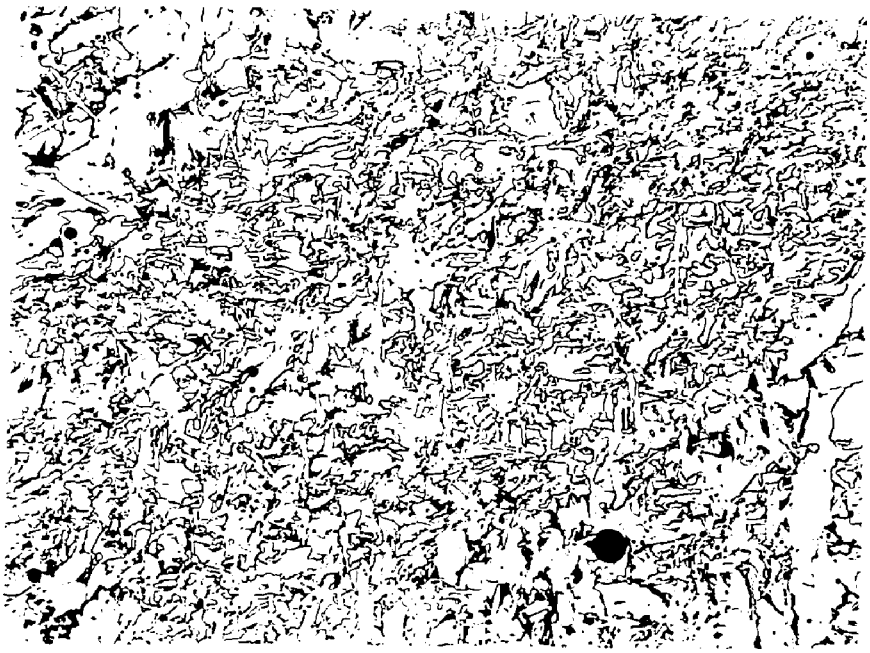

31B 1.27% Mn 27J @ -18 C Nital 500X Weld S062

Figure 31. Effect of Manganese on Microstructure

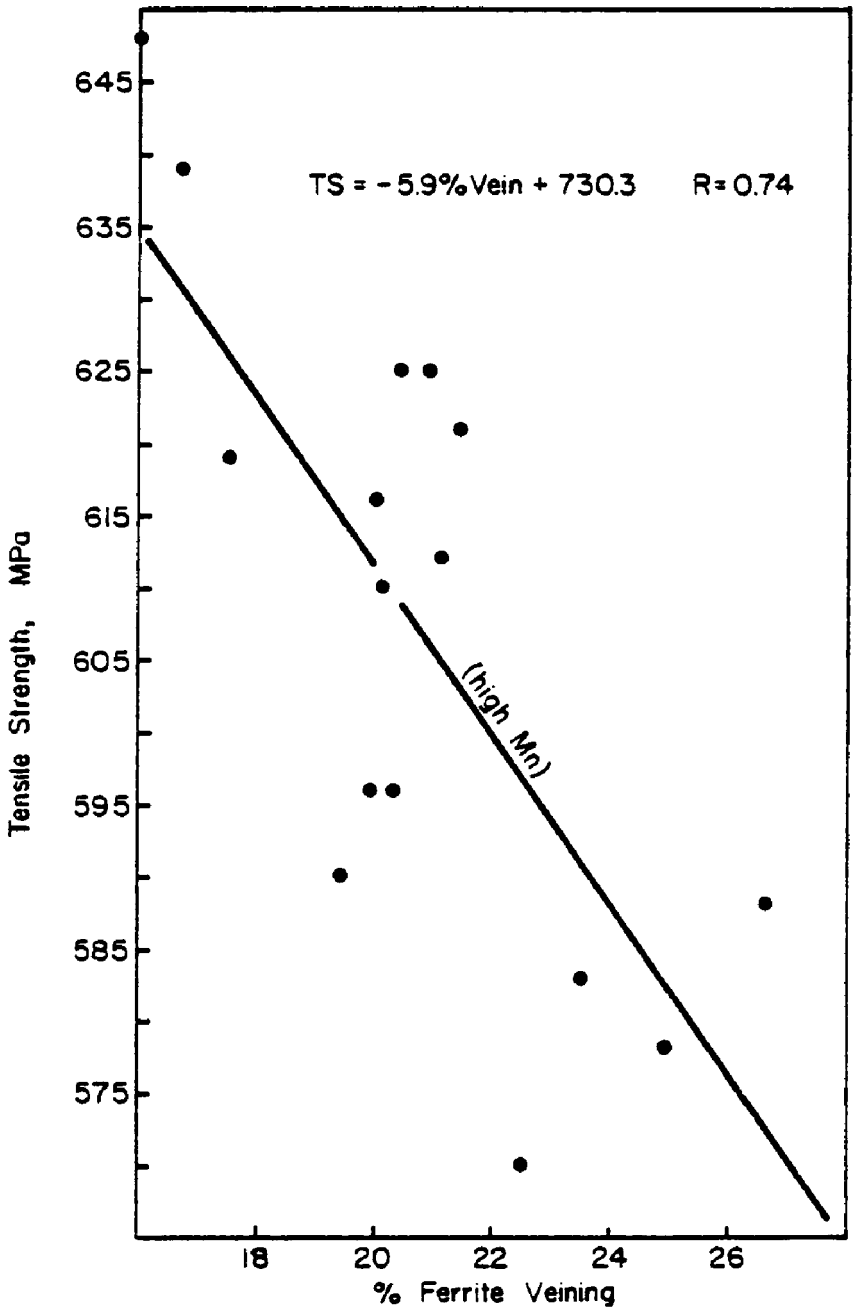

Figure 32. Tensile Strength Versus % Ferrite Veining. Manganese is nominally 1.3%. Equation is least squares fit.

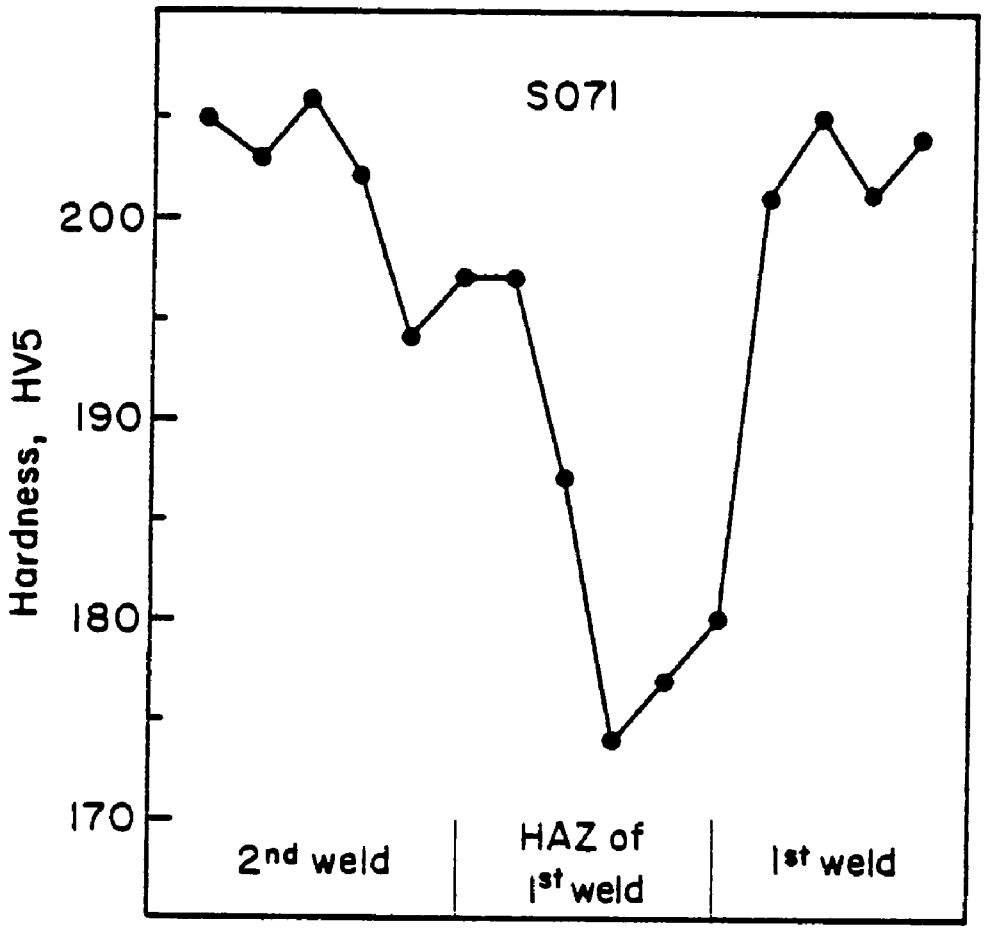

Figure 33. Hardness Versus Position in the Weld Deposit.

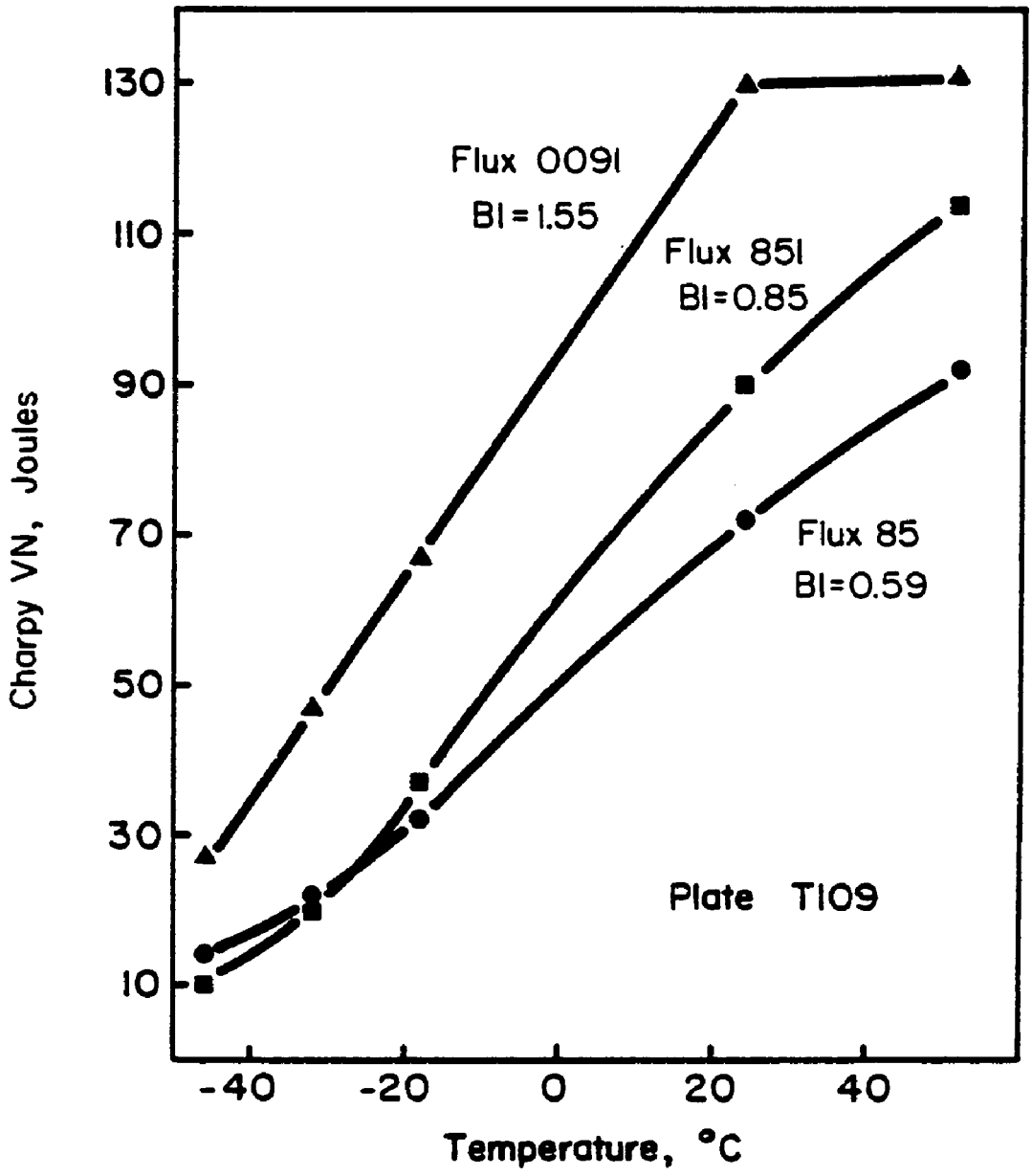

Figure 34. Charpy Energy Curves for 85, 851, and 0091 Fluxes.

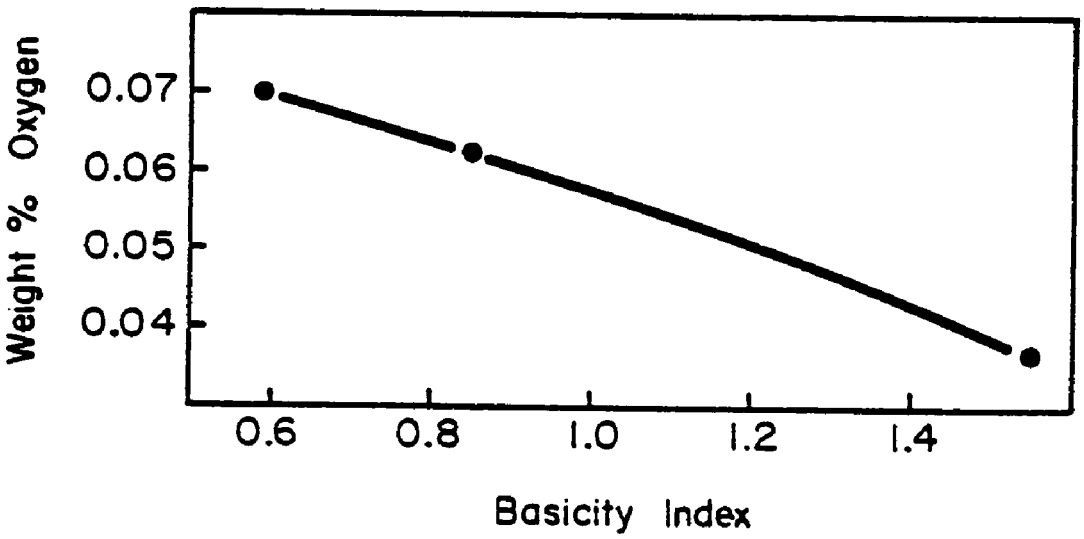

Figure 35. Oxygen Content of Weld Metal Versus Flux Basicity.

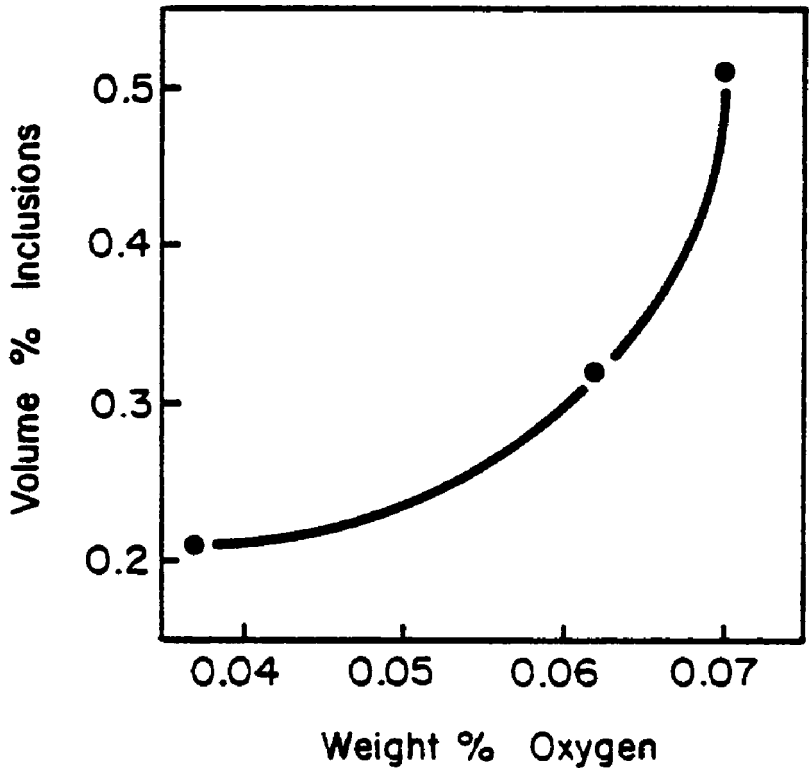

Figure 36. Volume of Inclusions Versus Weld Metal Oxygen Content.

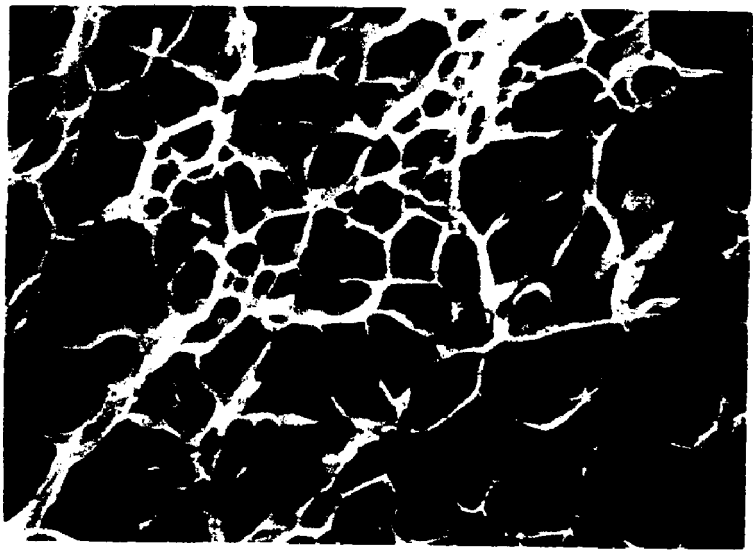

37A 0.070% O 92 J at +52 C 2000X Weld T109/85

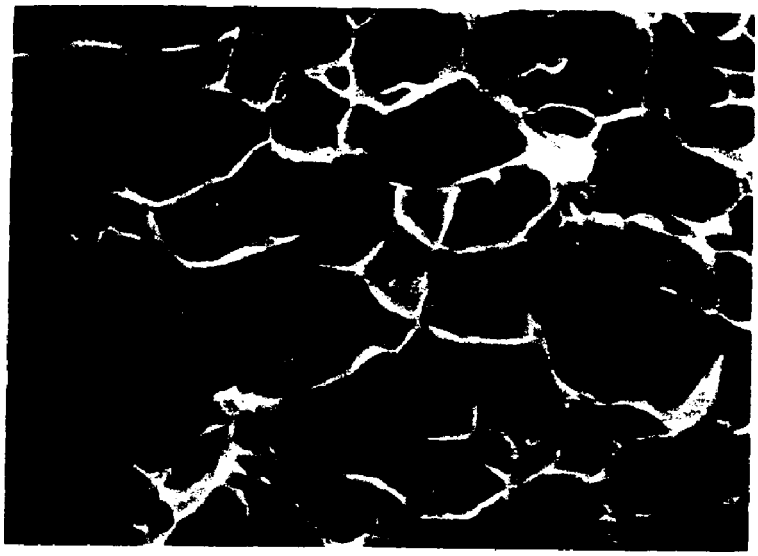

37B 0.037% O 131 J at +52 C 2000X Weld T109/0091

Figure 37. Scanning Electron Micrographs of Broken Charpy Specimens (52 C).

A 0.062% O 21.1% Veining Nital 200X Weld T109/851

B 0.037% O 15.3% Veining Nital 200X Weld T109/0091

Figure 38. Effect of Oxygen on Microstructure.

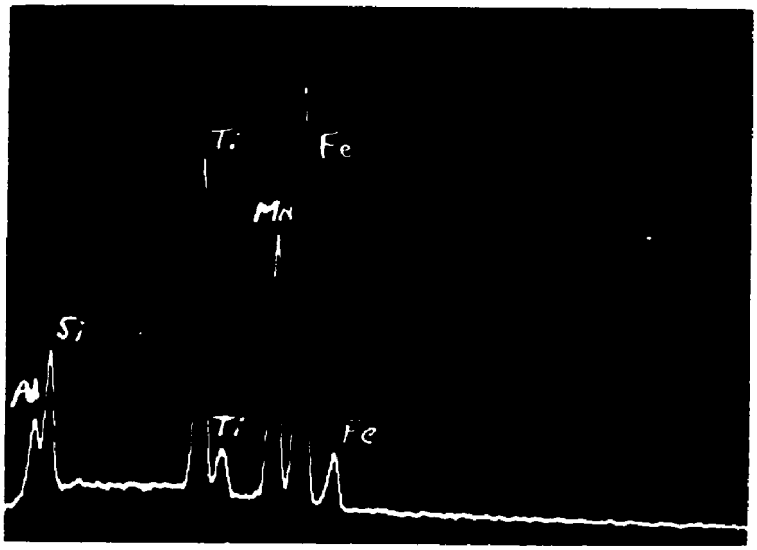

Figure 39. X-Ray Spectrum of an Oxide Particle on the Surface of a Broken Charpy Specimen.

40A 0.0% Mo 16.7% Veining Nital 100X Weld W059/123

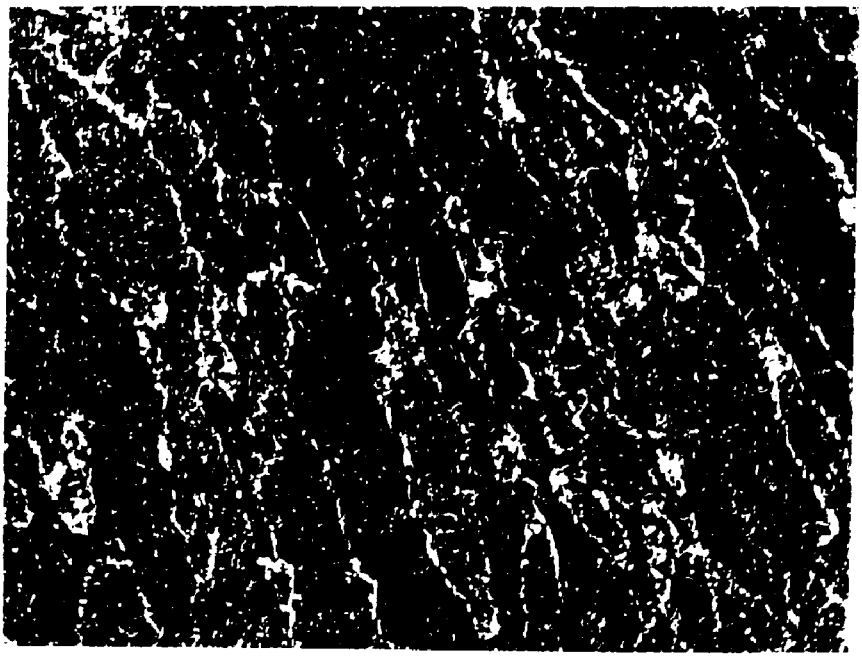

40B 0.15% Mo 3.8% Veining Nital 100X Weld W059/128

Figure 40. Effect of Molybdenum on Microstructure.

TABLE 1. BASE PLATE CHEMISTRIES

Plate	C	Mn	P	S	Si	Ti	Al
1-S087	0.150	1.45	0.004	0.005	0.27	0.066	0.030
2-S060	0.120	1.48	0.004	0.005	0.53	0.100	0.050
3-S069	0.065	1.42	0.003	0.006	0.44	0.075	0.043
4-T107	0.072	1.49	0.006	0.003	0.24	0.075	0.037
5-W007	0.078	1.44	0.012	0.005	0.27	0.280	0.041
6-S071	0.062	1.53	0.003	0.005	0.51	0.270	0.041
7-S062	0.130	1.47	0.003	0.004	0.48	0.310	0.045
8-S091	0.130	1.54	0.003	0.005	0.31	0.330	0.040
9-T109	0.098	1.50	0.007	0.004	0.33	0.170	0.040
10-S064	0.130	1.29	0.003	0.005	0.27	0.170	0.036
11-S061	0.120	1.44	0.004	0.004	0.48	0.190	0.048
12-S070	0.071	1.52	0.003	0.005	0.49	0.160	0.039
13-S095	0.071	1.40	0.006	0.003	0.28	0.150	0.033
14-S066	0.130	0.92	0.003	0.006	0.40	0.065	0.037
15-S092	0.120	0.93	0.003	0.006	0.49	0.210	0.030
16-S068	0.130	0.96	0.003	0.005	0.46	0.260	0.026
17-S093	0.073	0.89	0.003	0.005	0.46	0.150	0.021
18-S094	0.130	0.97	0.002	0.006	0.29	0.170	0.024
19-W024	0.110	1.45	0.007	0.003	0.35	0.039	0.036
20-W058	0.067	1.46	0.003	0.004	0.23	0.002	0.042
21-W059	0.150	1.51	0.003	0.004	0.40	0.002	0.050

TABLE 2. WELD METAL CHEMISTRIES

Weld	C	Mn	P	S	Si	Ti	Al	O	N
1-S087	0.120	1.15	0.008	0.014	0.38	0.029	0.012	0.082	0.009
2-S060	0.100	1.37	0.006	0.012	0.60	0.077	0.039	0.085	0.009
3-S069	0.083	1.12	0.008	0.015	0.48	0.038	0.019	0.087	0.010
4-T107	0.070	1.30	0.010	0.011	0.37	0.036	0.020	0.083	0.019
5-W007	0.072	1.33	0.012	0.012	0.39	0.150	0.017	0.081	0.010
6-S071	0.063	1.39	0.008	0.012	0.55	0.110	0.022	0.087	0.012
7-S062	0.110	1.27	0.005	0.011	0.54	0.160	0.016	0.062	0.011
8-S091	0.110	1.41	0.007	0.012	0.47	0.160	0.017	0.072	0.008
9-T109	0.094	1.30	0.010	0.012	0.46	0.058	0.019	0.070	0.013
10-S064	0.110	1.18	0.005	0.012	0.38	0.090	0.012	NA*	0.009
11-S061	0.099	1.37	0.003	0.011	0.49	0.140	0.014	NA	0.012
12-S070	0.073	1.28	0.010	0.013	0.58	0.062	0.021	NA	0.013
13-S095	0.068	1.30	0.003	0.013	0.38	0.071	0.017	NA	0.012
14-S066	0.110	1.06	0.005	0.012	0.45	0.041	0.012	0.076	0.008
15-S092	0.110	1.09	0.006	0.013	0.58	0.080	0.010	NA	0.009
16-S068	0.110	1.07	0.006	0.012	0.54	0.130	0.015	0.077	0.008
17-S093	0.078	1.04	0.005	0.013	0.52	0.078	0.016	NA	0.008
18-S094	0.120	1.03	0.004	0.012	0.43	0.084	0.020	NA	0.009
19-W024	0.090	1.29	0.010	0.014	0.47	0.025	0.020	0.077	0.012
20-W058	0.066	1.31	0.005	0.014	0.36	0.009	0.026	0.091	0.009
21-W059	0.130	1.33	0.005	0.012	0.50	0.010	0.033	0.079	0.014

* NA = Not Analyzed

Table 3. Weld Grouping and Elemental Ranges for Factorial Series

	CTS Series	CTM Series
	1-S087	2-S060
	2-S060	3-S069
	3-S069	6-S071
	4-T107	7-S062
	5-W007	11-S061
	6-S071	12-S070
	7-S062	14-S066
	8-S091	15-S092
	9-T109	16-S068
	10-S064	17-S093
	11-S061	18-S094
	12-S070	21-W059
	13-S095	
	19-W024	
	20-W058	
	21-W059	
Carbon	0.063-0.13	0.063-0.13
Manganese	1.29ave(1.12-1.39)	1.04-1.39
Silicon	0.36-0.60	0.52ave(0.43-0.60)
Titanium	0.009-0.16	0.010-0.16

TABLE 4. RESULTS OF REGRESSION ANALYSIS

CTS Series: $Variable = B_0 + B_1(C) + B_2(Ti) + B_3(Si) + B_{11}(C^2) + B_{22}(Ti^2) + B_{33}(Si^2) + B_{12}(CTi) + B_{32}(SiTi) + B_{31}(SiC)$

CTM Series: $Variable = B_0 + B_1(C) + B_2(Ti) + B_3(Mn) + B_{11}(C^2) + B_{22}(Ti^2) + B_{33}(Mn^2) + B_{12}(CTi) + B_{32}(MnTi) + B_{31}(MnC)$

Variables:
1) YSW - weld metal yield strength
2) TSW - weld metal tensile strength
3) -46W - weld metal CVN energy at -46C
4) -32W - weld metal CVN energy at -32C
5) -18W - weld metal CVN energy at -18C
6) +24W - weld metal CVN energy at +24C
7) +52W - weld metal CVN energy at +52C
8) 20JTT - CVN 20J transition temperature
9) 55JTT - CVN 55J transition temperature
10) MWH - maximum weld metal hardness HV5
11) % V - % ferrite veining

Variable	Units	Coefficients of Equations										Statistical Parameters			
		B_0	B_1	B_2	B_3	B_{11}	B_{22}	B_{33}	B_{12}	B_{32}	B_{31}	R	SErr	P	Correlation
-- CTS Series --															
1 YSW	MPa	889.5	-10627.0	804.0	0	65758.8	0	812.0	12358.6	-3793.2	-4602.3	0.89	15.3	0.024	Good
2 TSW	MPa	707.3	- 3826.4	534.8	0	29372.0	0	332.0	0	- 696.8	-2269.7	0.92	11.1	0.003	Excellent
3 -46W	J	12.6	0	- 91.3	0	0	480.9	0	-417.1	0	109.9	0.89	1.7	0.002	Excellent
4 -32W	J	39.4	- 497.6	0	0	2208.3	- 498.4	- 27.8	0	0	382.6	0.96	1.8	0.001	Excellent
5 -18W	J	7.2	- 239.6	- 276.9	178.4	0	0	-254.9	0	474.1	519.2	0.91	2.1	0.005	Excellent
6 +24W	J	86.4	0	- 190.9	0	0	-5886.0	-222.3	0	0	2356.3	0.75	10.0	0.043	Good
7 +52W	J	156.9	- 1170.8	- 159.8	0	5007.4	0	0	983.0	0	0	0.86	4.4	0.010	Excellent
8 20JTT	°C	- 4.9	0	265.2	-140.7	0	0	178.4	0	- 349.6	- 157.2	0.92	2.9	0.001	Excellent
9 55JTT	°C	3.3	0	146.4	0	0	0	0	0	0	- 96.1	0.86	4.8	0.001	Excellent
10 MWH	HV5	178.6	219.4	314.4	0	0	0	0	-2232.3	0	0	0.82	4.8	0.003	Excellent
11 %V	%	-10.0	895.1	-106.5	-4.5	-5085.7	439.9	0	0	0	0	0.84	1.9	0.017	Good
-- CTM Series --															
11 YSW	MPa	-58.4	6475.9	0	424.3	0	4481.2	0	-9676.8	0	-4693.9	0.69	23.4	0.440	Poor
2 TSW	MPa	435.1	0	2357.5	0	9291.9	0	140.2	0	-1850.8	-1155.0	0.93	9.2	0.012	Good
3 -46W	J	-16.4	0	0	27.5	0	521.1	0	0	- 122.7	0	0.95	1.5	0.001	Excellent
4 -32W	J	0.3	0	- 310.9	27.9	0	1092.3	0	0	0	- 18.5	0.97	2.1	0.001	Excellent
5 -18W	J	76.1	0	-1373.7	- 27.6	0	1436.2	0	0	830.5	0	0.95	3.5	0.001	Excellent
6 +24W	J	134.2	0	-2270.0	- 38.0	0	1684.5	0	2005.3	1287.2	0	0.96	4.9	0.002	Excellent
7 +52W	J	-89.8	0	0	0	0	0	0	-1935.3	106.6	0	0.87	3.1	0.002	Excellent
8 20JTT	°C	-47.9	0	1429.4	0	0	-1978.5	0	0	- 740.3	0	0.95	5.1	0.001	Excellent
9 55JTT	°C	-43.2	0	2274.6	32.5	0	0	0	-3135.0	-1395.4	0	0.96	4.9	0.001	Excellent
10 MWH	HV5	175.5	0	0	23.1	0	0	0	321.2	0	0	0.74	3.7	0.028	Good
11 %V	%	58.9	-614.1	718.7	-37.7	0	-910.5	0	0	-405.1	497.9	0.97	1.7	0.005	Excellent

TABLE 5. ALL-WELD-METAL LONGITUDINAL TENSILE PROPERTIES

Weld	Yield Strength MPa	Tensile Strength MPa	% Elongation 12.7 mm	% Reduction of Area
1-S087	494	625	26.0	61.7
2-S060	492	621	25.0	61.3
3-S069	469	570	30.0	61.4
4-T107	449	578	30.0	64.1
5-W007	495	612	31.0	72.4
6-S071	519	619	OGM*	67.0
7-S062	500	625	34.0	67.1
8-S091	527	648	30.0	63.4
9-T109	470	596	32.0	60.9
10-S064	507	615	38.0	73.4
11-S061	450	596	30.0	63.5
12-S070	499	610	30.0	65.4
13-S095	488	590	28.0	62.8
14-S066	535	592	OGM	62.7
15-S092	514	609	32.0	72.4
16-S068	494	615	OGM	63.3
17-S093	482	586	28.0	64.4
18-S094	484	607	30.0	63.0
19-W024	452	588	41.0	63.5
20-W058	482	583	28.0	60.1
21-W059	523	639	32.0	58.2

* OGM = Broke Outside Gage Marks

Table 6. Weld Metal Toughness Data

Weld	Charpy V-Notch Energy, Joules					20 J Transition Temp., °C	55 J Transition Temp., °C
	-46C	-32C	-18C	+24C	+52C		
1-S087	13	26	30	66	NT*	-37	7
2-S060	14	21	32	64	90	-34	13
3-S069	12	20	31	72	85	-31	10
4-T107	NT	22	30	74	95	-37	10
5-W007	9	11	20	51	87	-16	26
6-S071	9	16	30	61	95	-25	17
7-S062	8	13	27	61	79	-25	18
8-S091	11	14	28	53	81	-25	27
9-T109	14	22	32	72	92	-34	7
10-S064	8	17	25	72	85	-24	12
11-S061	7	12	32	76	79	-25	9
12-S070	10	20	28	69	89	-32	12
13-S095	9	20	29	75	90	-32	7
14-S066	8	19	33	64	85	-30	12
15-S092	5	8	12	51	80	- 4	29
16-S068	5	5	10	34	75	+ 3	42
17-S093	5	10	13	43	89	- 5	34
18-S094	5	10	16	53	84	-11	24
19-W024	15	24	35	109	NT	-37	-1
20-W058	15	19	35	89	106	-30	-3
21-W059	18	30	35	81	88	-39	-4

* NT = Not Tested

Table 7. Weld Metal Hardness and Metallographic Data

Weld	Maximum Hardness HV5	% Ferrite Veining	% Retained Austenite	% Volume Inclusions
1-S087	209	20.4	3.0	0.64
2-S060	212	21.4	3.1	0.60
3-S069	208	22.5	1.7	0.56
4-T107	206	24.9	1.9	0.52
5-W007	219	21.1	2.5	0.61
6-S071	214	17.5	3.0	0.49
7-S062	213	20.9	1.9	0.56
8-S091	217	16.0	3.8	0.56
9-T109	204	19.9	3.3	0.51
10-S064	210	20.0	0.4	NM*
11-S061	206	20.3	0.7	NM
12-S070	203	20.1	1.8	NM
13-S095	198	19.4	1.0	NM
14-S066	200	18.9	0.8	NM
15-S092	201	24.7	0.2	NM
16-S068	206	32.4	0.8	NM
17-S093	199	29.3	1.0	NM
18-S094	204	27.6	0.6	NM
19-W024	196	26.6	2.1	0.59
20-W058	192	23.5	0.6	0.58
21-W059	205	16.7	2.3	0.62

* NM = Not Measured

Table 8. Structure Size of Acicular and Heat-Affected Zone Ferrite

Weld	Ti	Mn	Structure Size			
			Acicular		Heat-Affected Zone	
			u	ASTM	u	ASTM
W058	0.009	1.31	1.8	15.0	3.3	13.2
W059	0.010	1.33	2.1	14.5	3.5	13.0
T107	0.036	1.30	1.9	14.8	3.9	12.7
T109	0.058	1.30	2.0	14.7	3.8	12.8
S062	0.160	1.27	1.7	14.7	3.8	12.8
S066	0.041	1.06		NM*	4.2	12.5
S093	0.078	1.04		NM	4.3	12.4
S068	0.130	1.07		NM	4.2	12.5

*NM = Not Measured

Table 9. Results of the Regression Analysis for the Combined Chemistry and Metallographic Data Sets Versus Mechanical Properties

$$\text{Variable} = B_0 + B_1C + B_2Mn + B_3Si + B_4Ti + B_5\%V + B_6\%RA$$

20JTT = 20 joule transition temperature
55JTT = 55 joule transition temperature
MAX = maximum weld hardness
YSW = weld metal yield strength
TSW = weld metal tensile strength

Variable	B_0	B_1	B_2	B_3	B_4	B_5	B_6	R	SErr	P	Correlation
20JTT	-10.5	0	-40.1	0	150.8	1.1	0	0.89	5.8	0.001	excellent
55JTT	33.4	0	-40.0	0	188.3	0.7	0	0.90	5.8	0.001	excellent
MAX	200.3	44.4	4.4	0	89.2	-0.5	0	0.76	5.0	0.006	excellent
YSW	480.0	365.8	0	67.7	44.2	-2.6	0	0.62	21.6	0.09	fair
TSW	487.7	631.7	53.6	0	137.2	-0.8	0	0.82	12.8	0.001	excellent

Table 10. Weld Metal Chemistries and Data: Flux Variations

Weld/Flux	C	Mn	P	S	Si	Ti	Al	O	N	Flux Basicity
9-T109/85	0.094	1.30	0.010	0.012	0.46	0.058	0.019	0.070	0.013	0.59
9-T109/851	0.098	1.15	0.012	0.015	0.38	0.053	0.016	0.062	0.014	0.85
9-T109/0091	0.110	1.37	0.011	0.014	0.29	0.061	0.022	0.037	0.009	1.55

Weld/Flux	YS, MPa	TS, MPa	Average Hardness HV30	Charpy VN Energy, Joules				Transition Temperature		% Ferrite Veining	% Inclusions
				-46C	-18C	+24C	+52C	20J	55J		
9-T109/85	470	596	185	14	32	72	92	-34	7	19.9	0.51
9-T109/851	446	598	196	10	37	90	114	-32	-7	21.1	0.32
9-T109/0091	498	629	199	27	67	130	131	-51	-28	15.3	0.21

Table 11. Weld Metal Chemistries: Electrode Variations

Weld/Electrode	C	Mn	P	S	Si	Ni	Mo	Ti	Al	O	N
4-T107/123	0.070	1.30	0.010	0.011	0.37	NA*	NA	0.036	0.020	0.083	0.019
4-T107/128	0.080	1.20	0.007	0.007	0.35	NA	0.03	0.054	0.025	NA	0.020
4-T107/130	0.089	1.25	0.004	0.009	0.36	0.35	0.16	0.030	0.015	NA	0.013
7-S062/123	0.110	1.27	0.005	0.011	0.54	NA	NA	0.160	0.016	0.062	0.011
7-S062/128	0.110	1.25	0.008	0.009	0.57	NA	0.04	0.140	0.023	NA	0.015
7-S062/130	0.130	1.31	0.004	0.010	0.49	0.37	0.16	0.090	0.014	NA	0.017
20-W058/123	0.066	1.31	0.005	0.014	0.36	NA	NA	0.009	0.026	0.091	0.009
20-W058/128	0.072	1.29	0.007	0.010	0.37	NA	0.15	0.009	0.039	NA	0.012
21-W059/123	0.130	1.33	0.005	0.012	0.50	NA	NA	0.010	0.033	0.079	0.014
21-W059/128	0.130	1.36	0.004	0.009	0.51	NA	0.15	0.010	0.045	NA	0.014

* NA = Not Analyzed

Table 12. Weld Metal Data: Electrode Variations

Weld/Electrode	YS, MPa	TS, MPa	Hardness HV30	Charpy VN Energy, Joules -46C	-18C	+24C	+52C	55 J Transition Temp., °C	% Ferrite Veining
4-T107/123	449	578	183	NT*	30	74	95	10	24.9
4-T107/128	546	646	208	19	36	69	NT	8	16.5
4-T107/130	503	627	199	19	54	84	NT	-16	10.8
7-S062/123	500	562	198	8	27	61	79	18	20.9
7-S062/128	478	576	219	24	27	69	NT	15	10.5
7-S062/130	546	696	220	28	37	78	NT	11	7.1
20-W058/123	482	583	183	15	35	89	106	-3	23.5
20-W058/128	544	623	202	29	64	109	103	-25	7.2
21-W059/123	523	639	201	18	35	81	88	-4	16.7
21-W059/128	596	696	215	28	49	94	98	-10	3.8

* NT = Not Tested

REFERENCES

1. Meyer, L., et.al., "Titanium As A Strengthening And Sulfide-Controlling Element In Low-Carbon Steels," Processing And Properties of Low-Carbon Steels (Edited by M. Gray), Cleveland, 1973, AIME.

2. Yoshino, Y. and Stout. R. D., "Effect Of Microalloys On The Notch Toughness Of Line Pipe Seam Welds," Welding Journal, March 1979, 58(3) Research Suppl., p. 59s.

3. Garland, J. G. and Kirkwood, P. R., "Metallurgical Factors Controlling Weld Metal Toughness In The Seam Welding Of Line Pipe," Brit. Steel Corp. Rep., GS/PROD/832/176/C.

4. Sawhill, J. M. and Wada, T., "Properties Of Welds In Low-Carbon Mn-Mo-Cb Line Pipe Steels," Welding Journal, January 1975, 54(1) Research Suppl., p. 1s.

5. Levine, E. and Hill, D. C., "A Review Of The Structure And Properties Of Welds In Columbium Or Vanadium Containing High Strength Low Alloy Steels," WRC Bulletin No. 213, February 1976.

6. Bauman, S. F., et.al., "Wire And Flux Development For Seam Welding Of HSLA Line Pipe," WRC Monograph, Welding Of Line Pipe Steels, March 1977, p. 56.

7. Kirkwood, P. R., "Microstructural And Toughness Control In Low Carbon Weld Metals," Metal Construction, May 1978, p.260.

8. Signes, E. G. and Baker, J.C., "Effects Of Columbium And Vanadium On The Weldability Of HSLA Steels," Welding Journal, June 1979, 58(6) Research Suppl., p. 179s.

9. Rittinger, J. and Fehervari, A., "The Influence Of Microalloying Elements On The Toughness Of Steels In Welded Structures," Proceedings Of Microalloying 75, 1975, p. 88.

10. Bernard, G., "A View-Point On The Weldability Of Carbon-Manganese And Microalloyed Structural Steels," Proceedings Of Microalloying 75, 1975, p. 52.

11. Hart, P. H. M., et.al., "The Weldability Of Microalloyed Steels," Proceedings Of Microalloying 75, 1975, p. 41.

12. Thomas, R. D., "Submerged-Arc Welding Of HSLA Steels," Metal Progress, April 1977, 111(4), p. 30.

13. Ito, Y. and Nakaniski, M., "Study On Charpy Impact Properties Of Weld Metal With Submerged-Arc Welding," Sumitomo Search No. 15, May 1976, p.42.

14. Widgery, D. J., "Deoxidation Practice And Toughness Of Mild Steel Weld Metal," Welding Research International, 1974, 4(2), p. 54.

15. Boniszewski, T., "Titanium In Steel Wires For CO_2 Welding," Metal Construction, May 1969, 1(3), p. 225.

16. Jessman, J. R., "Columbium Pickup In High-Dilution, Submerged-Arc Weld Deposits," Proceedings of Microalloying 75, 1975, p. 74.

17. Slutskaya, T. M., et.al., "Effects Of The Manganese And Titanium Contents Of Electrode Wires On The Mechanical Properties Of Submerged-Arc Welds," Auto. Welding, January 1971, 21(1), p. 35.

18. Still, J. R. and Rogerson, J. H., "The Effects Of Titanium And Boron Additions To Multipass Submerged-Arc Welds In 50D Plate," Metal Construction, July 1978, p. 44.

19. Brodskii, A.Y. and Tsniisk, R. P., "The Effects Of Titanium On The Weldability Of The Low-Alloy 14G2T Steel," Auto. Welding, 1964, 86, p. 13.

20. Comstock, G. F., et.al., Titanium In Steel, Pitman Publishing Corp., New York, 1949.

21. Mandel'berg, S. L., et.al., "Effects Of Titanium On The Properties Of Welded Joints In Silicon-Manganese Steel," Auto. Welding, 1972, 25, p. 7.

22. Patchett, B. M., et.al., "Welding Low Temperature Containment Plant," Welding Institute Conference, London, November 20-22, 1973.

23. Borisenko, M. M. and Novozhilov, N. M., "Effects Of Titanium On The Impact Toughness Of The Weld Metal Of CO_2 Joints," Welding Production, 1974, 21(1), p. 36.

24. Kotecki, D. J. and Moll, R.A., "A Toughness Study Of Steel Weld Metal From Self-Shielded Flux-Core Electrodes," Welding Journal, March 1972, 51(3), Research Suppl., p.138s.

25. Gensamer, M., "Strength And Ductility," Trans. ASM, 1964, 36, p. 30.

26. Widgery, D. J., "Deoxidation Practice For Steel Weld Metal," Welding Journal, March 1976, 55(3) Research Suppl., p. 57s.

27. Ouden, G. den, et.al., "Influence Of Chemical Composition On Mild Steel Weld Metal Notch Toughness," Welding Journal, March 1975, 54(3) Research Suppl., p. 87s.

28. Dorschu, K. E. and Stout, R. D., "Some Factors Affecting The Notch Toughness Of Steel Weld Metal," Welding Journal, March 1961, 40(3) Research Suppl., p. 97s.

29. Moll, R. A. and Stout, R. D., "Composition Effects In Iron-Based Weld Metal," Welding Journal, December 1967, 46(12) Research Suppl., p. 551s.

30. Sagan, S. S. and Campbell, H. C., "Factors Which Affect Low-Alloy Weld Metal Notch Toughness," WRC Bulletin No. 59, April 1960.

31. Dorschu, K. E., "Factors Affecting Weld Metal Properties In Carbon And Low-Alloy Pressure Vessel Steels," WRC Bulletin No. 231, October 1977.

32. Tuliani, S. S. and Farrar, R. A., "The Affects Of Silicon In Submerged-Arc Metals At Low Concentrations," Welding and Metal Fab., September 1975, p. 553.

33. Saunders, G. G., "Effect Of Major Alloying Elements On The Toughness Of High Strength Weld Metal," Welding Research International, 1972, 7(2), p. 91.

34. Sakaki, H., "Effect Of Alloying Elements On Notch Toughness Of Basic Weld Metals," Journal of the Japan Welding Society, September 1959, 28(9), p.610.

35. Garland, J. G. and Kirkwood, P. R., "The Notch Toughness Of Submerged-Arc Weld Metal In Microalloyed Structural Steels," IIW Document IX-892-74, 1974.

36. Tiluani, S. S., "Notch Toughness Of Commercial Submerged-Arc Weld Metal," Welding and Metal Fab., August 1969, 38(8), p. 327.

37. Hughes, P.C., "Notch Toughness Of Submerged-Arc Welds-Part 2," Welding Institute Research Report, March 1968, 26/1968/M.

38. Wilms, G.R., "Toughness Differences Between Silicon-Killed And Semi-Killed Steel Plate," Journal of Aus. Ins. of Metals, December 1973, 18(4), p. 182.

39. Bailey, N. and Davis, M. L. E., "Fluxes For Submerged-Arc Welding Ferritic Steels--A Literature Survey," Welding Institute Research Report, May 1977, 38/1977/M.

40. Jackson, C. E., "Fluxes And Slags In Welding," WRC Bulletin No. 190, December 1973.

41. Duren, C. F., et.al., "Development Of Welding Technique For Longitudinal Welded Large-Diameter Pipe Production," WRC Monograph, Welding of Line Pipe Steels, March 1977, p. 3.

42. Takahashi, N., et.al., "Developments For Seam Welding Of High Test Line Pipe," WRC Monograph, Welding of Line Pipe Steels, March 1977, p. 36.

43. Dolby, R. E., "Factors Controlling Weld Toughness--The Present Position: Part 2, Weld Metals," Welding Institute Research Report, May 1976, 14/1976/M.

44. Levin, E. and Hill, D. C., "Structure-Property Relationships In Low-C Weld Metal," Met. Trans. A, September 1977, 8A, p. 1453.

45. Garland, J. G. and Kirkwood, P. R., "Towards Improved Submerged-Arc Weld Metal," Metal Construction, June 1975, 7(6), p. 320.

46. Widgery, D. J. and Saunders, G. G., "Microstructures In Steel Weld Metals," Welding Institute Research Bulletin, October 1975, 16(10), p. 277.

47. Abson, D. J. and Dolby, R. E., "Microstructural Transformations In Steel Weld Metals," Welding Institute Research Bulletin, July 1978, 19(7), p. 202.

48. ----------, Strategy Of Experimentation, E. I. DuPont de Nemours and Co., 1974.

49. ----------, Statistics For The Engineer, SAE SP-250, 1973.

50. Cullity, B. D., Elements Of X-Ray Diffraction, Addison-Wesley Publishing Company, Inc., 1976.

51. Stout, R. D., "Hardness As An Index Of The Weldability And Service Performance Of Steel Weldments," WRC Bulletin No. 189, November 1973.

52. BMDP2R, A Computer Program For Multiple Stepwise Regression Analysis, UCLA Biomedical Division, 1975.

53. F-Distribution, A Computer Program For Evaluating The P-Statistic, Hewlett-Packard, 1974.

54. Thaulow, C., "Comparison Between COD At Initiation Of Ductile Crack Growth And Maximum Load Of Submerged-Arc Weld Metal," Int. Jour. Of Fracture, 1979, 15, p.R31.

55. Rose, A. and Hougardy, H., Atlas Zur Warmebehandlung der Stahle: Band 2, Verlag Stahleisen M.B.H., Dusseldorf, 1972.

56. Bain, E. C. and Paxton, H.W., Alloying Elements In Steel, American Society for Meatls, Metals Park, Ohio, 1966.

57. Hertel, J. and Robush, G., "The Transformation Behavior Of Low Pearlite Steels With Titanium Additions," Archuv Fur Das Eisenhuttenwessen, 1977, 48(6), p. 329.

58. Rhines, F. and DeHoff, R. T., Quantitative Microscopy, McGraw Hill Publishing Company, Inc., 1968.

59. Alasaarela, P. and Saarinen, A., "The Effect Of Carbon, Manganese, And Silicon On The Austenite Content Of The Heat-Affected Zone In Structural Steels," Scand. J. Met., 1(1972), p. 127.

60. Woodyatt, L. R., "A Study Of The Iron-Chromium-Molybdenum-1% Carbon System At 870 C," Ph.D. Dissertation, 1975.

61. Kriege, O. H., "Metallography--A Practical Tool For Correlating The Structure And Properties Of Materials," ASTM-STP 557, 1973, p. 220.

62. Garland, J. G. and Bailey, N., "The Formulation And Properties Of Submerged-Arc Welding Fluxes," Brit. Steel Corp. Rep., GS/PROD/498/1/74/C.

63. Broek, D., "Roll Of Inclusions In Ductile Fracture," Engineering Fracture Mechanics, 1973, 5(1), p. 55.

64. Eriksson, K. "Fracture Toughness And The Distribution Of Inclusions," Scand. Jour. of Met., 1975, 4, p. 173.

65. Ito, Y., et.al., "Effect Of CaF_2 In Flux On Toughness Of Weld Metal," Sumitomo Search No. 16, November 1976, p. 78.

66. North, T. H., et.al., "Notch Toughness Of Low Oxygen Content Submerged-Arc Deposits," Welding Journal, December 1979, 58(12) Research Suppl., p. 343s.

67. Blake, P. D., "Oxygen In Steel Weld Metals," Metal Construction Construction, March 1979, 11(3), p. 118.

68. Garland, J. G. and Kirkwood, P. R., "A Reappraisal Of The Relationship Between Flux Basicity And Mechanical Properties In Submerged-Arc Welding," Welding and Metal Fabrication, April 1967, p. 217.

69. Abson, D. J., et.al., "The Role Of Non-Metallic Inclusions In Ferrite Nucleation In Carbon Steel Weld Metals," Trends in Steel and Consumables for Welding, London, November 14, 1978, p. 75.

70. Cochrane, R. C. and Kirkwood, P. R., "The Effect Of Oxygen On Weld Metal Microstructure," Trends in Steel and Consumables for Welding, London, November 14, 1978, p. 103

VITA

The author was born in Reading, Pennsylvania on November 5, 1948; he is the son of Dorothy W. and James P. Snyder.

Mr. Snyder received his elementary and secondary education in the public school system of Reading, Pennsylvania and received a Bachelor of Arts degree in Physics from Kutztown State College. In 1973, the author received a Master of Science degree in Metallurgy and Materials Science from Lehigh University. His thesis, which was completed under the direction of Dr. R. W. Kraft, was entitled "The Effects of Sulfur and Heat Treatment on the Solidification Structures of High Speed Tool Steel." During his Master's work, the author held teaching and research assistantships.

Since graduating from Lehigh University, Mr. Snyder has been employed as a research engineer in the Research Department of the Bethlehem Steel Corporation. The author's primary area of research is welding metallurgy.

The author is a member of the American Welding Society, the American Society for Metals, and the University Research Committee of the Welding Research Council.